Dissociation of the nuclear basket triggers chromosome loss in aging yeast

Mihailo Mirkovic[1], Jordan McCarthy[1], Anne Cornelis Meinema[1], Julie Parenteau[2], Sung Sik Lee[1,3], Sherif Abou Elela[2], Yves Barral[1]

1-Institute of Biochemistry, Department of Biology, ETH Zürich, Zürich, Switzerland
2- Département de microbiologie et d'infectiologie, Faculté de médecine et des sciences de la santé, Université de Sherbrooke, Sherbrooke, QC, Canada
3-Scientific Center for Optical and Electron Microscopy, ETH Zürich, Switzerland

ABSTRACT:

In many organisms, aging is a clear risk factor for chromosome mis-segregation, the main source of aneuploidy. Here, we report that old yeast cells lose chromosomes by partitioning them asymmetrically to their daughter cells together with the pre-existing (old) spindle pole body (SPB, centrosome equivalent in yeast). Strikingly, remodelling of the nuclear pore complex (NPC) and the displacement of its nuclear basket triggered these asymmetric chromosome segregation events. Simultaneously, nuclear basket displacement caused unspliced pre-mRNAs to leak into the cytoplasm. We show that removing the introns of three genes involved in chromosome segregation was sufficient to fully suppress chromosome loss in old cells. Promoting pre-mRNA leakage in young cells also caused asymmetric chromosome partitioning and loss through the same three introns. Therefore, we propose that basket displacement from NPCs and its consequences for pre-mRNA quality control are key triggers of aging phenotypes such as aneuploidy.

INTRODUCTION

Cellular aging results in conserved phenotypes, including chromosome mis-segregation, fragmentation of mitochondria, accumulation of damaged or misfolded proteins, and alteration of nuclear morphology[1-3]. Importantly, the nuclear pore complex (NPC) is remodelled in aging across evolutionary lineages, as shown in fungi, worms, and mammals [4-6]. As the primary gateway between the nucleus and cytoplasm, the NPC controls mRNA export and protein distribution between these two cellular compartments. The most prominent change in the NPCs of old cells is the loss of their nuclear basket, which lies on the nucleoplasmic side of the NPC. Nuclear basket loss is observed both in dividing cells and upon expression of the progeric variant of Lamin A, progerin[8-9]. The protein TPR (Mlp1 and Mlp2 in *S. cerevisiae*) is the main structural component of the nuclear basket in mammals. The nuclear basket serves as a critical processing hub for mRNA export and nuclear retention of pre-mRNA, protein quality control and gene regulation[10-15]. Altering the structure or function of the NPC or its nuclear basket could have diverse and wide-ranging effects on cellular function given the NPC's broad range of functions and central position in eukaryotic cellular information flow. Despite this and the fact that the reorganization of NPC architecture with age is prominent in a wide range of organisms, little is known about whether and how NPC remodelling contributes to aging.

The unicellular fungus *Saccharomyces cerevisiae*, budding yeast, is a remarkably useful system for studying the role of NPCs in cellular aging[1,3]. Budding yeast undergoes replicative aging, during which

39 the mother cell produces a finite number of daughter cells before dying[16]. After the mother cell enters
40 senescence, the rate of cell division slows. Importantly, several studies have emphasized that the yeast
41 NPC is remodelled during replicative aging[4-6], but the exact consequences of its reorganization are not
42 fully understood.

43 Extrachromosomal DNA circles (also called eccDNAs) accumulate in the mother cell nucleus and are
44 one of the key drivers of aging in the budding yeast[7-9]. These DNA circles form during the cell's lifetime
45 through excision of genomic segments, generally by recombination between repeated sequences[10]. The
46 vast majority of these circles (>99%) stems from the highly repetitive rDNA locus and are referred to as
47 extrachromosomal rDNA circles (ERCs)[7]. As the cell age, these circles accumulate exponentially
48 because they are replicated in S-phase and retained in the mother cell at mitosis[7,11]. By the end of their
49 life, yeast cells contain about 1000 ERCs, which represents roughly the same amount of DNA as the
50 rest of the genome[11]. Importantly, their retention in the mother cell relies on their anchorage to NPCs
51 via the acetyltransferase complex SAGA[5,12]. These NPC-ERC units are then confined to the mother part
52 of the dividing nucleus by a lateral diffusion barrier forming in the nuclear envelope in the future plane
53 of cleavage[12-14]. Yeast cells undergo a closed mitosis, meaning that they keep their nuclear envelope
54 intact throughout mitosis. Remarkably, anchorage of ERCs to NPCs results in the dissociation of their
55 nuclear basket, which is a direct result of SAGA-driven acetylation of nucleoporins on the nucleoplasmic
56 side of the NPC, including Nup60[12]. Consequently, most of the NPCs of old yeast cells lack a nuclear
57 basket[5]. However, it is unknown whether nuclear basket displacement has consequences for the
58 physiology and survival of the cell or contributes to the aging process.

59 One way to approach the question of whether nuclear basket displacement from the NPCs contributes
60 to the aging process is to determine whether other aging phenotypes depend on basket displacement
61 and if so, how. In this study, we focused on chromosome instability in old yeast cells as a case study
62 of an aging phenotype. In many metazoans, including humans, aging results in increasing frequency
63 of chromosome mis-segregation and aneuploidy, correlating with increasing risk of cancer[15,16]. Our
64 understanding of the molecular mechanisms of chromosome segregation errors in old cells remains
65 rudimentary. Here, we report evidence that NPC remodelling during yeast aging leads to chromosome
66 loss from old mother cells and characterize the underlying mechanisms.

67 **RESULTS**

68 **Aging yeast cells lose chromosomes**

69 To examine whether aging affects the karyotype of yeast cells, we visualized and followed the fate of
70 individual chromosomes in replicatively aging mother cells, using either TetO-labelled chromosome II or
71 chromosome IV as reporters. Chromosome IV is the second longest chromosome, while chromosome
72 II is of average size. Both chromosomes were labelled with an array of 256 TetO repeats in the vicinity
73 of their centromere[17,18]. These chromosomes were visualized by expressing fluorescently tagged
74 versions of the TetR protein, which binds to TetO repeats (TetR-GFP or TetR-mCherry; Figures 1A-B).
75 We then monitored budding yeast mother cells throughout their entire replicative lifespan using live-
76 imaging microscopy combined with a microfluidics platform[5,19]. The replicative age of each mother cell
77 was measured by counting the number of daughters that it budded off over time, defining how many

78 budding events they have already completed at a given time point (completed budding events, CBE).
79 Bud size and the number and position of the spindle pole bodies (SPBs, labelled with mCherry) were
80 used to identify the cell cycle stages at which the cells were imaged (Figure 1A).

81 Analysis of these images showed that all young mother cells (~0-3 CBE; t=0h) and their daughters
82 contained a fluorescent dot, documenting the presence of the labelled chromosomes in all of them.
83 However, when reaching the age of 18 to 22 CBE (t=24h), 10-15% of these now old mother cells had
84 lost their dot (Figures 1B-C). This was observed irrespective of which chromosome was labelled, and
85 which fluorescent tag was used. Fluorescence of the labelled SPB was not affected, indicating that dot
86 loss was not caused by fluorophore instability in old cells. A chromosome dot could be lost from aging
87 mother cells in three possible ways: 1) Chromosome mis-segregation during anaphase 2) Migration of
88 the entire nucleus into the daughter cell 3) Through the loss of a TetO array. The SPB is located in the
89 nuclear envelope, so the presence of the SPB but the absence of the chromosome points to
90 chromosome loss during anaphase, rather than the mis-segregation of the entire nucleus into the
91 daughter cell (Figure 1A). Nuclear mis-segregation into the daughter cells was previously reported
92 during replicative aging and is marked by the segregation of both SPBs to the daughter compartment
93 (Sup Figure 1A-B)[20]. While we do observe whole nuclei mis-segregation in ~3% of the cells, this is a
94 distinct event from chromosome loss, which occurs in ~10-15% of final replicative divisions.

95 To test if the loss of fluorescent chromosomal foci was due to the loss of the TetO array specifically or
96 of the entire chromosome, we included a second label (an array of 256 repeats of the LacO sequence)
97 in the middle of the long arm of chromosome IV (Figure 1B) and asked whether the cells that lost the
98 TetO array lost the LacO repeats as well. Analysis of these images showed that 85% of the cells lacking
99 the TetO array had indeed lost the LacO array (50/59). Thus, these cells had probably lost the entire
100 chromosome. Supporting this notion, loss of the TetO array was fatal to the cells. More than 99%
101 (145/146 chromosome II loss events) of the dot-less cells failed to divide further, as expected for a
102 haploid cell losing an entire chromosome. Thus, chromosome loss took place specifically in the last
103 division of old mother cells and likely caused their death.

104 Finally, we examined whether the loss of a reporter chromosome points to general chromosome
105 instability in old cells. To assess this possibility, we quantified how often aging cells simultaneously lost
106 both chromosome II and chromosome IV (Figure 1B-C). As expected, the co-loss rate (~5%) was lower
107 than the individual loss rates (~10-15%), but notably higher than the ~1% expected by chance alone.
108 Therefore, the loss of a single chromosome does not necessarily accompany the loss of another, but
109 the high rate of simultaneous mis-segregation points to general chromosome instability in old cells.
110 Considering that the budding yeast haploid genome has 16 chromosomes, the high loss frequency of a
111 single chromosome and the fact that individual chromosomes are lost in not fully independent manners
112 we estimate that 35-70 % of aging mother cells likely lose several chromosomes in their final division,
113 whereas the other cells die with an intact karyotype. We concluded that much like many other organisms,
114 yeast undergoes a burst of chromosome instability in old age (Figures 1A, C).

115

116 In contrast to chromosomes, extra-chromosomal DNA circles accumulate in the yeast mother cell with
117 age rather than being lost[7,12] . Similarly, deleting the centromere from a chromosome causes the
118 retention of both sister chromatids in the mother cell[18]. Thus, we wondered whether centromeres drive
119 chromosome loss in old mother cells. DNA circles containing a centromeric sequence (*CEN*) were lost
120 from aged mother cells at a similar rate to full-size chromosomes (~20% of old cells; Figures 1B-C).
121 Removing the centromere of the exact same circle was shown in previous work to cause its retention in
122 the mother cell rather than its loss[5,12,13]. Therefore, centromeres are necessary and sufficient for
123 chromosomes and mini chromosomes to be lost from aging mother cells. To exclude the possibility that
124 the TetO array used to label them is the cause of chromosome and mini-chromosome loss in aging, we
125 also characterized the stability of a circular mini-chromosome expressing short-lived GFP as a marker
126 instead of TetO repeats. Scoring of the GFP signal demonstrated that old mother cells lost these mini-
127 chromosomes at essentially the same frequency as they lose the TetO labelled one (Figures 1B-C). We
128 concluded that centromeres drive chromosome loss in old cells.

129 **Aged cells asymmetrically partition both sister chromatids to the bud**

130 Given the prominent role of the centromere in chromosome loss, we rationalized that the loss of
131 chromosomes in old mother cells could be due to mitotic mis-segregation events. To determine whether
132 it was the case, we next focused our analysis on cells imaged during mitosis in time-lapse recordings of
133 aging cells (Figure 2A). Analysis of anaphases in old mother cells revealed a striking increase in the
134 frequency of chromosome mis-segregation, using labelled chromosome II, IV and minichromosome as
135 reporters (Figure 2B). In 600 total anaphase events captured in our movies we found that 66 (11%) of
136 them co-segregated the labelled sister chromatids to a single pole with, 54/66 (82%) of the mis-
137 segregation events resulting in asymmetric partition of the chromatids to the bud of these old mother
138 cells (Figure 2C). This was virtually never observed in young cells (Figure 2A-B). Remarkably, the
139 frequency of chromosome loss in the old mother cells and of sister chromatids segregating
140 asymmetrically to the bud were in the same size order, irrespective of whether chromosome II or
141 chromosome IV was labelled. Therefore, chromosome loss from old mother cells seems fully explained
142 by a rise in sister chromatid non-disjunction with age, resulting in co-segregation of the sister chromatids
143 asymmetrically to the bud. Next, we examined the mechanism behind this peculiar mode of directed
144 chromosome mis-segregation.

145 In budding yeast, the pre-existing (old) SPB, which the cell inherited from the previous mitosis,
146 segregates in a highly biased manner to the bud (~95% of mitoses)[21-23]. Consequently, labelling of stable
147 SPB components, such as the core SPB protein Spc42, with mCherry causes the pre-existing SPB to
148 shine bright and segregate in 95% of mitoses to the bud (Figure 2A, red arrowhead), while the new one
149 is dim and remains in according proportions in the mother cell. This useful effect is a result of the folding
150 kinetics of mCherry. In short, mCherry matures slowly (~45 minutes half-time) relative to the duration of
151 yeast mitosis (~50 minutes from spindle assembly to completion of cytokinesis), and therefore the new
152 mCherry-labelled SPB is dimmer than the old one. Given the mother-daughter bias of SPB inheritance
153 and sister chromatid mis-segregation with age, we wondered whether the non-disjoining sister
154 chromatids of old cells attach to and co-segregate with the old SPB. Thus, we examined the partition of
155 the labelled chromosomes relative to the pre-existing and new SPBs in old mother cells (t=24h, Figures

156 2D, E). In about 10% of old cells, SPB inheritance is inverted, meaning that the old SPB goes to the
157 mother cell instead of the daughter[21,22]. In a strong majority of these cases (80%), the non-disjoining
158 sister chromatids followed the old SPB to the mother cell, instead of going to the bud (Figures 2D, E).
159 We conclude that non-disjoining sister chromatids of old mother cells remained attached to the pre-
160 existing SPB and partitioned with it to the bud, causing them to lose these chromosomes. In other words,
161 SPB identity mattered more than mother-daughter identity in determining which cell inherited the mis-
162 segregated chromosomes.

163 In budding yeast, sister chromatids both initially attach to the pre-existing SPB, which is available first.
164 These syntelic attachments are then dissolved by the aurora B kinase, allowing sister chromatids to
165 reorient, reach bi-orientation and partition symmetrically in mitosis[24,25]. Failure to correct these initial
166 attachments errors causes sister chromatids to co-segregate with the old SPB to the bud[26]. The similarity
167 between this phenotype and the mechanism of chromosome loss in old mother cells suggested,
168 therefore, that the error correction pathway might be impaired in old yeast cells. To test this possibility,
169 we analysed the effects of dampening the function of aurora B (called Ipl1 in budding yeast) during
170 aging. Young cells carrying the temperature sensitive *ipl1-321* mutant allele and grown at a permissive
171 temperature (27°C) showed no detectable chromosome loss (Figure 2F). However, they started losing
172 chromosomes early in age (Figure 2F), resulting in a shortened lifespan (Sup Fig 1C). Strikingly, the
173 chromosome loss frequency of the old *ipl1-321* mutant cells (t=24h) was indistinguishable from that of
174 the wild type cells, indicating that the effects of age and reducing Ipl1 activity were not additive (Figure
175 2F). This suggests that age and the *ipl1-321* mutation affect the same pathway. We concluded that old
176 cells lose chromosomes due to defects in correcting chromosome attachment errors.

177 **ERC accumulation drives chromosome loss in aging**

178 To identify mechanisms behind the deterioration of mitotic error correction with age, we investigated
179 whether chromosome loss is causally linked to other aging events, particularly to the displacement of
180 the basket from NPCs[5]. Given that basket displacement is triggered by accumulating ERCs and their
181 SAGA-dependent anchorage to NPCs[5,12,13], we first investigated whether ERC accumulation promotes
182 chromosome loss. Mutant cells lacking the deacetylase Sir2, which inhibits recombination in the rDNA
183 locus, form ERCs at an increased rate, accumulate them quicker, and their replicative lifespan is shorter
184 than that of wild type cells[7,27]. Supporting the notion that ERC accumulation might promote chromosome
185 loss, these mutant cells also showed a strong and premature loss of the reporter chromosome (Figure
186 3A). To further test the effect of ERC accumulation, we asked whether reducing their formation rate
187 delays chromosome loss. Recombination in the rDNA locus is stimulated by the presence of a replication
188 fork barrier between rDNA units[28]. While these barriers prevent the transcription machinery to collide
189 with replication forks coming from neighbouring rDNA units, the stalling forks are fragile, causing high
190 rates of double strand breaks. Therefore, removing these fork barriers, for example by inactivating the
191 fork barrier protein Fob1, drastically decreases the rate at which ERCs form and accumulate, stabilizes
192 the nuclear baskets of NPCs and prolongs the life span of the cells[5,28]. Strikingly, the *fob1*Δ mutant cells
193 trapped in our microfluidics platform lost chromosome II at a substantially reduced frequency compared
194 to wild type cells, even after dividing 20 times or more (Figure 3A). Introducing an artificial replicative
195 DNA circle with a different sequence than an ERC into wild type cells also promoted chromosome loss,

196 supporting the idea that DNA circles promote chromosome loss with age independently of their
197 sequence (see below). Taken together, the chromosome loss rates seen in cells with artificial DNA
198 circles, along with those in *sir2*Δ and *fob1*Δ cells, show that chromosome loss correlates well with the
199 accumulation of extrachromosomal DNA circles. Since the primary known effect of DNA circle
200 accumulation is to cause the displacement of the nuclear basket from NPCs, we wondered next whether
201 this event was causally linked to chromosome loss. Supporting this notion, removal of the SAGA subunit
202 Sgf73, which mediates ERC attachment to NPCs and the subsequent displacement of their nuclear
203 basket, phenocopied the effect of the *fob1*Δ mutation[12]: the *sgf73*Δ mutant cells failed to show any
204 significant increase in chromosome loss frequency at any age (Figure 3A). Thus, our data suggested
205 that ERC formation and anchorage to NPCs triggered chromosome loss in old yeast cells.

206 **Nuclear basket remodelling drives chromosome loss**

207 To investigate whether basket displacement promotes chromosome loss in some manner, we next
208 perturbed the nuclear basket and measured whether this accelerated chromosome loss and aging. To
209 do this, we disrupted the *MLP1* gene, encoding the major isoform of the structural basket protein TPR
210 in yeast. In stark contrast to the *sgf73*Δ and *fob1*Δ single mutants and the wild type cells, the *mlp1*Δ
211 single mutant cells exhibited a rapid increase in chromosome loss frequency as they aged, as
212 determined by using our reporter chromosome II, along with a shortened replicative lifespan (Figures
213 3A-B). Thus, our data suggest that displacement of the basket from NPCs as the cells age promotes
214 chromosome loss through some yet unknown mechanism.

215 **Introns in genes of the aurora B pathway drive asymmetric chromosome partitioning in aging**

216 Together our data suggested that the displacement of the nuclear basket from NPCs upon ERC
217 anchorage weakened the molecular pathway that corrected chromosome attachment errors (Figure 3A).
218 This impaired ability to correct erroneous chromosome attachments in turn caused old mother cells to
219 lose chromosomes to their buds. To test this hypothesis, we next investigated how basket displacement
220 could lead to asymmetric chromosome partitioning. The basket of the nuclear pore has been involved
221 in various processes, such as mRNA export[29], protein quality control[30], docking of environmentally
222 regulated genes to the nuclear periphery upon their induction[31], the retention of faulty mRNAs in the
223 nucleus, such as unspliced pre-mRNAs[32,33], as well as docking Mad1 and Mad2, two key components
224 of the mitotic spindle assembly checkpoint (SAC), to the NPC[34,35].

225 The SAC components Mad1 and Mad2 bind Mlp1, Mlp2 and Nup60 at the basket of NPCs[35]. However,
226 basket dissociation, which delocalizes Mad1/2 from the nuclear periphery, does not appear to interfere
227 with their function[35]. Nevertheless, we investigated whether SAC dysfunction could account for aging
228 phenotypes caused by basket dissociation and for the premature aging phenotype seen in *mlp1*Δ mutant
229 cells. Arguing against this hypothesis, the *mad1*Δ and *mad2*Δ single mutant cells exhibited no change
230 in replicative lifespan compared to wild type cells and did not phenocopy *mlp1*Δ mutant cells (Sup Fig
231 2A). Therefore, we searched for other mechanisms through which basket displacement could trigger
232 chromosome loss.

233 While perusing the list of genes involved in chromosome segregation (Figure 4A) we noticed that only
234 three of them contain an intron, *NBL1*, *MCM21* and *GLC7*. Surprisingly, these three genes all function
235 with Ipl1/aurora B in preventing syntelic chromosome attachment. Nbl1/borealin is a component of the
236 chromosome passenger complex of which aurora B/Ipl1 is the catalytic subunit. Mcm21/CENP-O is a
237 docking receptor for Ipl1/aurora B at kinetochores. Glc7/PP1A is the protein phosphatase 1, which
238 counteracts aurora B by dephosphorylating its targets at the outer-kinetochore[36-38]. Intrigued by this
239 remarkable convergence, we wondered whether asymmetric chromosome partitioning in aging could
240 stem from the presence of these three introns in error correction genes. We rationalized that
241 displacement of the basket from NPCs could potentially affect the regulation, export and hence
242 expression of intron-containing transcripts, specifically, thereby affecting the function of the *NBL1*,
243 *MCM21* and *GLC7* genes.

244 To investigate the possibility that they contribute to the high rate of chromosome loss in old cells, we
245 removed the introns of *GLC7, MCM21, NBL1* (*-Δi* alleles) and imaged these mutant cells throughout
246 their replicative lifespan, monitoring chromosome II segregation. Removing each intron individually or
247 all three simultaneously (*3xΔi* strain) had no detectable effects on chromosome segregation in young
248 cells (Figure 4B), cell growth and mitotic timing (Sup. Figure 3A-C), Interestingly, whereas the removal
249 of *GLC7*'s intron decreases the expression of the gene by about 50% and affects cell proliferation [39-41],
250 we note that the *GLC7-Δi* allele is duplicated in our strain, probably owing to recombination between
251 transposon LTRs surrounding it (Sup Figure 3E-F). We suspect that this duplication explains why our
252 *GLC7-Δi* mutant strain grew as well as wild type cells. Simultaneously removing all three introns nearly
253 completely suppressed chromosome loss in old cells (Figure 4B-C). Removing them individually or in
254 pair did so as well, albeit the effects were milder. Importantly, the simultaneous removal of *NBL1*,
255 *MCM21* and *GLC7* introns did not affect the duration of the last budding event (Sup Figure 3D), indicating
256 that it suppressed chromosome loss without alteration cell cycle progression. Removing the introns of
257 the two α-tubulin genes *TUB1* and *TUB3* simultaneously had no effect, indicating that the observed
258 effects were specifically related to the introns of *NBL1*, *MCM21* and *GLC7* and not to introns in general
259 (Figure 4B). The effects observed were similar for chromosome II and chromosome IV, indicating that
260 the role of these introns was not chromosome specific (Sup Figure 2B). Furthermore, removing these
261 three introns also suppressed the occurrence of asymmetric anaphases in old cells (Figure 4C),
262 supporting the view that asymmetric chromosome segregation and chromosome loss go hand-in-hand
263 and are under the control of these three introns. Strengthening this conclusion, removal of these introns
264 also suppressed chromosome loss in the *ipl1-321* mutant cells (Sup Figure 1D).

265 Remarkably, simultaneous removal of *MCM21*, *NBL1* and *GLC7* introns had also a substantial effect on
266 the longevity of the cells, extending their replicative lifespan up to ~20% (Figure 4D). A similar effect
267 was observed in the *ipl1-321* mutant cells (Sup Fig1C). Thus, chromosome loss may indeed be the first
268 direct cause of death for many yeast cells upon aging, although other mechanisms eventually take over
269 when chromosome loss is abrogated.
270
271
272

273 **Basket destabilization causes intron-dependent chromosome loss in young cells**

274 Our data were consistent with the hypothesis that basket dissociation from NPCs promotes chromosome
275 loss through an intron-dependent dampening of the error correction pathway. To test this hypothesis in
276 greater depth we asked whether mutations affecting the nuclear basket also promote chromosome loss
277 outside of the aging context. Thus, we characterized chromosome segregation in young *mlp1*Δ cells
278 (Figure 5A-C). Analysis of chromosome II segregation indicated that the *mlp1*Δ mutant cells not only
279 exhibited a four-fold increase in their chromosome mis-segregation frequency compared to the young
280 wild type cells, but ~80% of these mis-segregation events followed the old SPB, as in old cells (Figure
281 5C). Furthermore, this chromosome loss was suppressed upon removal of the introns of *MCM21*, *NBL1*
282 and *GLC7* (Figure 5B). Therefore, although to a lower extent than in old cells, defects in the nuclear
283 basket result in asymmetric chromosome partitioning in an intron-dependent manner in young cells as
284 well. Interestingly, removal of these three introns also rescued the age dependent chromosome loss
285 and partially restored the longevity of the *mlp1*Δ mutant cells (Figure 5D-E). We concluded that intron-
286 dependent dampening of the error correction pathway is one, even if not the only progeric effects of the
287 *mlp1*Δ mutation. Possibly, other introns promote additional aging phenotypes. Thus, we conclude that
288 basket displacement promotes chromosome loss in young mutant cells and old wild type mother cells.

289 **Intron deletion suppresses the effect of DNA circle accumulation on chromosome loss**

290 As seen above, chromosome loss correlates well with conditions that promote ERC accumulation and
291 their anchorage to NPCs. This idea gained in traction as we progressed, because ERC attachment, and
292 the attachment of any DNA circle, to NPCs is known to mediate nuclear basket displacement[5].Thus, we
293 further investigated the relationships between DNA circle accumulation and chromosome loss by
294 investigating how the removal of *NBL1*, *MCM21* and *GLC7* introns affected chromosome loss observed
295 upon DNA circle accumulation. For this, we followed two parallel approaches. First, we tested whether
296 introducing a replicative DNA circle into the cells is sufficient to drive chromosome loss during aging,
297 and if so, whether this event required the presence of the introns of *NBL1*, *MCM21* and *GLC7*. Thus,
298 we transformed the wild type and the *3x*Δ*i* mutant strains carrying the labelled chromosome II as reporter
299 with the yeast replicative plasmid YRp17[42]. We then monitored the frequency at which these transformed
300 cells lost the reporter chromosome as they underwent aging. YRp17 contains a replication origin (*ARS1*)
301 but no centromere, such that it accumulates in the mother cells with each replicative cycle (Figure 6A).
302 As expected[7], the cells carrying YRp17 showed a much shorter lifespan (10 CBE median RLS, Figure
303 6B). Remarkably however, the effect of YRp17 on longevity was substantially suppressed by the 3xΔi
304 mutations (Figure 6B). Analysis of chromosome loss indicated that introducing this DNA circle promoted
305 chromosome loss, starting early in life and increasing rapidly with age (Figure 6C). Furthermore, removal
306 of the introns of *NBL1*, *MCM21* and *GLC7* (*3x*Δ*i* cells) largely suppressed the effect of YRp17 on
307 chromosome loss. However, note that the suppressive effect of the *3x*Δ*i* mutations on longevity and
308 chromosome loss was only partial, indicating that YRp17 promotes chromosome loss through both a
309 mechanism that involves these three introns, and at least one additional mechanism independent of
310 these introns.

311 As a second approach, we investigated whether removing the introns of *NBL1*, *MCM21* and *GLC7*
312 mitigates the chromosome loss phenotypes of the *sir2*Δ mutant cells. Supporting this hypothesis, the
313 *3x*Δ*i* triple mutation significantly, though modestly, improved the longevity phenotype of these cells
314 (Figure 6D). As in cells carrying YRp17, the triple intron removal indeed ameliorated the premature
315 chromosome loss phenotype of the *sir2*Δ mutant cells (Figure 6E). As for YRp17, the effect of the 3xΔi
316 was substantial and significant, but partial. Thus, we concluded that the accumulation of DNA circles,
317 such as ERCs and others, which promote the dissociation of the basket from NPCs and thereby drive
318 chromosome loss at least in part through the introns of *NBL1*, *MCM21* and *GLC7.* While this effect
319 appeared to be the dominant one in physiologically aged cells, additional effects seem to further promote
320 chromosome loss in the *sir2*Δ mutant cells and cells carrying an exogenous DNA circle, such as YRp17.

321 **Old cells leak pre-mRNA to the cytoplasm**

322 Putting our different observations together, our data suggested that removal of the nuclear basket from
323 NPCs in response to the accumulation of DNA circles with age causes old yeast mother cells to lose
324 chromosomes to their last bud. Furthermore, the effect of nuclear basket removal from NPCs was
325 primarily mediated by three introns. This suggested that the nuclear basket of NPCs enforces proper
326 chromosome segregation through its function in pre-mRNA processing or quality control. To test this
327 possibility, we next investigated whether old mother cells show defects in pre-mRNA quality control.
328 Since, basket mutant cells fail to retain unspliced pre-mRNAs in the nucleus [32,33], we reasoned that old
329 yeast mother cells also might leak pre-mRNAs to the cytoplasm.

330 As a first proof of principle, we characterized the localization of intronic RNA sequences in young and
331 old cells, using single molecule RNA fluorescence in situ hybridization (smRNA FISH). Most yeast
332 introns are short (50-150 nucleotides) and well below the minimal size detectable by smRNA FISH (>500
333 nts, ideally >1 kb). In the yeast genome, only 20 introns are longer than 500 nucleotides. Thus, we
334 created probes for the longest introns, namely those of *DBP2* (766 nts) and *YRA1* (1002 nts), and of
335 *GLC7* because of its role in chromosome segregation (525 nts). The introns of *NBL1* (66 nts) and
336 *MCM21* (88 nts) are too short for smRNA FISH. Cohorts of old cells were collected using the mother
337 enrichment program (MEP)[43] followed by FACS sorting to reach high homogeneity (see methods). By
338 inducing cell death in the daughter cells specifically, the MEP ensures that aging mother cells are diluted
339 linearly instead of exponentially in the population, greatly facilitating the isolation of very old cells. FACS
340 sorting ensured that the cohorts were free of young cells and young cell debris. With each of these three
341 series of smRNA FISH probes, we detected one or two nuclear foci in young cells (Figure 7A). Only very
342 few cells ((<3%) showed a focus in the cytoplasm. No foci were detected upon deleting the
343 corresponding introns (Δi), demonstrating probe specificity (Sup Figure 4A-B). In contrast, for each of
344 the three introns tested, smRNA FISH detected intronic RNA sequences in the cytoplasm of most old
345 cells. This was not due to an increase in overall smRNA FISH foci number during aging (See Sup Figure
346 4C), but due to the change in foci distribution between nucleus and the cytoplasm. For example, in the
347 case of *GLC7,* ~70% of smRNA FISH foci were found in the cytoplasm of old mother cells, compared to
348 ~3% in young cells (Figure 7A-B). Thus, 3 out of 3 tested introns showed a strong tendency to leak to
349 the cytoplasm in old mother cells. However, this first test did not clarify whether the full pre-mRNA or
350 only the intron escaped from the nucleus.

351 To directly address this question, we turned to a functional assay and monitored the translation of an
352 unspliced pre-mRNA reporter in the cytoplasm. This fluorescent reporter contains the coding sequence
353 for mCherry in the intron and expresses GFP upon proper splicing of the nascent transcript. Therefore,
354 mCherry is only translated when the unspliced pre-mRNA leaks out of the nucleus (Figure 7C)[44]. Cells
355 carrying this construct integrated at the *TRP1* locus were trapped and imaged in our microfluidics
356 platform. As cells aged, we measured the number of completed budding events and the fluorescence
357 levels of the two reporter fluorophores. Fluorescence signal analysis established that the mCherry/GFP
358 ratio increased in old compared to young cells, demonstrating elevated pre-mRNA translation in the
359 cytoplasm of a large majority of aged cells (Figures 7D-E).

360 Consistent with ERC-dependent leakage and translation of this reporter, the mCherry/GFP ratio
361 increased prematurely and to a higher level in the *sir2*Δ mutant, compared to the wild type cells (Figures
362 7D-F). The fact that signal was already observable in young *sir2*Δ mutant cells suggests that the
363 pleiotropic functions of Sir2 cause a fraction of these effects. Conversely, the *fob1*Δ mutant cells showed
364 a lowered mCherry/GFP ratio, which did not increase much during their lifespan (Figures 7D-F). Thus,
365 we conclude that ERC formation and accumulation promotes pre-mRNA leakage during yeast aging, as
366 expected from their effect on the nuclear basket.

367 **Pre-mRNA leakage causes intron-dependent chromosome loss in young cells**

368 Given the results above, we wondered whether chromosome loss in old cells is linked to their failure to
369 retain pre-mRNAs in the nucleus. Thus, we asked whether inducing pre-mRNA leakage in young cells
370 would trigger chromosome loss. The two yeast SR-protein Gbp2 and Hrb1 have been implicated in the
371 retention of pre-mRNAs in the nucleus by binding intron-containing transcripts and delaying their export
372 until they are properly spliced or degraded[45,46]. Accordingly, the *hrb1*Δ *gbp2*Δ double mutant cells leak
373 pre-mRNA to the cytoplasm at a higher rate than wild type cells[45,47]. Thus, we asked whether these
374 double mutant cells lost the labelled chromosome II at an increased frequency. As a control, we asked
375 whether the *snu66*Δ mutation, which affects the spliceosome itself directly[48,49], lead to similar
376 phenotypes.

377 The young spliceosome-defective *snu66*Δ mutant cells did exhibit a five-fold elevated level of
378 chromosome mis-segregation compared to young wild type cells. However, this mis-segregation was
379 not biased towards any specific SPB (Figures 8A-B), suggesting that it involved a distinct mechanism
380 than that observed in old cells and in young cells lacking the basket protein Mlp1. In contrast to the
381 *snu66*Δ mutant, the *hrb1*Δ *gbp2*Δ double mutant cells, showed an even further increased frequency of
382 chromosome mis-segregation, which was more than ten-fold above that of young wild type cells (Figure
383 8A). Furthermore, sister chromatid mis-segregation was strongly biased towards the old SPB (Figure
384 8B). Removing the introns of *GLC7, MCM21* and *NBL1* suppressed this chromosome segregation defect
385 (Figure 8A). Therefore, pre-mRNA leakage is sufficient to induce asymmetric chromosome partitioning
386 and is contingent on the presence of introns in the error correction genes *NBL1*, *MCM21* and *GLC7*.
387 The fact that mutations affecting the spliceosome did not promote asymmetric chromosome segregation
388 to any specific SPB with age indicates that the chromosome loss observed in old cells is not due to
389 splicing defects.

390 We conclude that accumulation of extrachromosomal DNA causes the displacement of the NPC basket
391 and subsequent leakage of pre-mRNAs. Leakage of intron-containing transcripts into the cytoplasm
392 impairs correction of syntelic attachments by the Ipl1/aurora B pathway, likely because three genes
393 involved in this pathway contain introns. This results in asymmetric partitioning of sister chromatids, and
394 age-associated chromosome loss. In summary, basket displacement and pre-mRNA leakage impair
395 error correction via an as-yet unknown mechanism involving the introns of *NBL1*, *MCM21* and *GLC7*.

396 **DISCUSSION**

397 Aging manifests itself through a broad diversity of conserved cellular phenotypes, but in most cases, we
398 know little about how these are causally linked to each other[1-3]. In this study we investigated whether
399 NPC remodelling in old yeast cells contributed to the emergence of other aging phenotypes, using
400 chromosome loss as a case study[5]. We showed that NPC remodelling is both necessary and sufficient
401 to drive the age-associated increase in chromosome loss and we identified the mechanisms involved.
402 Specifically, interventions that promoted displacement of the NPC basket, or basket defects more
403 broadly, enhanced non-disjunction and mis-segregation of sister chromatids to the bud, thereby
404 promoting chromosome loss in old yeast cells. These interventions included mutations that stimulated
405 ERC formation and removed the main yeast TPR isoform, Mlp1. Conversely, interventions that
406 prevented NPC remodelling, such as delaying ERC accumulation or preventing their anchorage and the
407 recruitment of SAGA to NPCs, restored proper chromosome segregation in old cells and supressed
408 chromosome loss. Thus, NPC remodelling appeared to be the pivotal point for triggering chromosome
409 loss in old cells.

410 Two potential caveats should be considered. First, the *sir2*Δ and *fob1*Δ mutations each have effects
411 beyond influencing ERC formation rates. The *sir2*Δ mutant cells lose silencing of the hidden mating type
412 loci, genetically behaving as diploids. They fail to silence subtelomeric regions and act through some
413 as-yet unknown mechanism on the maintenance of proteostasis[50-53]. Likewise, the *fob1*Δ mutation
414 renders the rDNA locus unstable, which might interfere with rRNA transcription and ribosome
415 biosynthesis[54]. However, their only clear common denominator is that they both affect ERC formation,
416 and hence NPC remodelling even if in opposite manners[27,28]. Moreover, the *sgf73*Δ mutation
417 phenocopies the effects of the *fob1*Δ mutation. Here again the only known functional overlap between
418 Fob1 and Sgf73 is that they promote ERC accumulation in the mother cell indirectly (Fob1) or directly
419 (Sgf73), ERC anchorage to NPCs and the consequent displacement of NPC basket[5,12]. Finally,
420 introducing another DNA circle in the form of a non-centromeric replicative plasmid, a process that also
421 causes basket displacement[5], promoted chromosome loss as well. Thus, our data establish that DNA
422 circle accumulation and attachment to NPCs trigger chromosome loss. Destabilizing the basket
423 independently of DNA circle accumulation also promotes the premature onset of chromosome loss,
424 indicating that it is the basket displacement from NPCs that triggers chromosome loss upon DNA circle
425 accumulation.

426 A second possible caveat is that chromosome loss could be linked to aging in some other manner. To
427 address this possibility, we investigated the molecular mechanisms that link basket displacement and
428 chromosome loss. Our data reveal that chromosome loss is due to the non-correction of syntelic

429 chromosome attachments in old cells. In young cells, the kinase aurora B and its accessory factors
430 enforce such corrections[24]. Our data also show that the inhibition of error correction in old cells requires
431 the presence of three introns, those of the genes *NBL1*, *MCM21* and *GLC7*. These three genes are the
432 only chromosome segregation machinery genes that contain an intron. Strikingly, the proteins Nbl1,
433 Mcm21 and Glc7 are all involved in the error correction pathway, together with aurora B/Ipl1[36-38].
434 Removing their introns restored proper attachment correction and chromosome segregation in old cells
435 and supressed the premature chromosome loss phenotype of the *ipl1-321* mutant cells grown at semi-
436 permissive temperature. Intron removal delays cell death but does not abrogate aging. Furthermore,
437 removing these introns not only supresses chromosome mis-segregation in old wild type cells, but also
438 in young *mlp1*Δ mutant cells. Thus, intron removal separates aging and chromosome loss, indicating
439 that these introns are part of the proximal cause of chromosome loss and act independently of age.
440 Therefore, our data indicate that there is a direct, intron-dependent link between basket displacement
441 from NPCs and chromosome loss. Our data indicate that this link involves the leakage of unspliced pre-
442 mRNAs out of the nucleus upon basket removal and affects the basket's function in mRNA quality
443 control. The fact that another, independent set of mutations that also interfere with pre-mRNA retention
444 in the nucleus, such as the *gbp2*Δ *hrb1*Δ double mutant cells, also increase the frequency of
445 chromosome loss through the same three introns strengthens this conclusion. Thus, together our data
446 establish that displacement of the nuclear basket from NPCs in old mother cell directly triggers
447 chromosome non-disjunction and loss through causing the leakage of the pre-mRNAs of the intron
448 containing genes *NBL1*, *MCM21* and *GLC7*.

449 This conclusion has several consequences and opens new questions. The key question stems from our
450 observation that releasing pre-mRNA from the nucleus relaxes the control that cells impose on
451 chromosome attachment. The question is, how does this work? Does it involve the translation of the
452 pre-mRNAs in the cytoplasm? Does it come about through the correlated loss of properly mature
453 mRNAs and hence, the reduced expression of their products? Two arguments speak against these
454 interpretations. First, if any of these two options were to account for the effect of pre-mRNA leakage,
455 mutations affecting splicing efficiency would lead to the same effects. However, tempering with the
456 spliceosome does not affect the correction of chromosome attachment errors to any extent and
457 specificity close to the effects of pre-mRNA leakage. Second, since Mcm21 and Glc7 have opposite
458 effects on chromosome correction it is unclear how impairing the expression of both would lead to the
459 synergistic effects that we observe between them. Finally, analysis of RNA-seq data from replicatively
460 aged cells indicate that if aging indeed impairs the splicing of some transcripts, such as those encoding
461 ribosomal proteins, it stimulates that of others[55]. This suggests that aging has a non-linear effect on
462 intron-containing transcripts. It will be important to determine whether basket displacement contributes
463 to these effects, how it does so and whether this could explain the effect it has on the error correction
464 pathway.

465 Our observation that basket displacement has such profound and highly specific impacts on processes
466 functionally very distant from that of the NPC, such as chromosome segregation, has several
467 consequences as well. First, it means that NPC remodelling could affect many more cellular functions
468 than only chromosome segregation. Interestingly, beyond mRNA quality control the basket of the NPC

469 is also involved in protein quality control and the activation of environmentally regulated genes, two
470 processes that are impaired in old cells[1,2]. Thus, basket displacement might contribute to these
471 phenotypes in aging cells. It is also very likely that the role of the basket in mRNA quality control could
472 affect more than only chromosome segregation. Curiously, while budding yeasts have kept only a subset
473 of the introns of their ancestors, these introns are not distributed randomly and seem to be enriched in
474 very specific processes, such as genes coding for ubiquitin-conjugating enzymes and proteasome
475 subunits, components of the mitochondrial respiratory chain and ribosomal proteins[56]. Interestingly,
476 decay of the ubiquitin-mediated protein degradation, mitochondrial membrane potential and of ribosome
477 assembly are classical and ubiquitous hallmarks of aging[1-3]. Thus, it is possible that basket displacement
478 in old cells contributes to the emergence of these aging phenotypes as well.

479 A second type of consequences emerging from our observations stems from the fact that displacement
480 of the NPCs' basket is also observed in stressed cells and not solely in the context of aging. For example,
481 heat shock also causes basket displacement in yeast[57]. Therefore, it is possible that the downstream
482 effects we observe in old cells also take place during stress response. In this respect, it is interesting to
483 note that heat shock has been associated with a strong rise in aneuploidy in yeast[58-60]. Furthermore,
484 aneuploidy is a common response to environmental stress and a primary mechanism for the emergence
485 of stress resistant clones in fungi[61]. Therefore, it is tempting to speculate that the chromosome mis-
486 segregation resulting from basket displacement might be a selected response to stress. It might be
487 selectively advantageous for cells to actively promote karyotype variations when their survival is in
488 question. It is therefore worth considering that a similar process, perhaps using similar mechanisms,
489 underlies the aneuploidy of cancer cells.

490 Third, the role of basket displacement in the emergence of aging phenotypes is likely not a peculiarity
491 of yeast. Using proteomics, basket displacement has been inferred to take place in aging cells such as
492 the hepatocytes of old mice and humans[62,63]. Little is known about whether the nuclear basket of
493 metazoans plays a similar role in pre-mRNA retention in the nucleus as that of yeast, but it is striking
494 that intron-retention is one of the hallmarks of aging on the metazoan transcriptome, and that pre-mRNA
495 processing genes are important for mitotic stability[64-67]. Intron retention would be expected if some
496 transcripts escaped the nucleus prematurely. More strikingly, perhaps the most ubiquitous effect of the
497 expression of the progeric variant of lamin A, progerin, across cell types is the displacement of the
498 nuclear basket protein TPR from NPCs[68]. We know still very little about the impact of basket
499 displacement in the aetiology of the Gilford-Hutchinson Progeria Syndrome, but our study suggest that
500 it might be relevant. If so, investigating the potential effects of progerin on pre-mRNA leakage might
501 become an essential step towards understanding how progerin expression causes premature aging.

502 In a broader sense, our findings might bring fundamental insights towards our understanding of aging.
503 For decades, the role of ERCs in aging has been perceived as a yeast peculiarity. However, the effect
504 it has on NPCs may close the gap. On one hand, it seems to illuminate what might be the commonality
505 between ERC-driven aging in yeast and other aging processes in other eukaryotes. Indeed, the basket-
506 centric view of aging that we propose here would explain how ERCs actually cause aging in yeast and
507 indicate that while ERC accumulation might be a yeast idiosyncrasy, its downstream effects are not. On
508 the other hand, this idea open two corollary questions. 1) What is the biological significance of eccDNAs

promoting basket displacement in yeast? 2) What causes basket displacement in other aging systems? We are intrigued by the idea that ERCs and any replicating eccDNA for that matter are the closest mimics that laboratory yeast strain may encounter of pathogenic DNA of exogenous origin. In that perspective, basket displacement and the ensuing effects might have first appeared as a response to infections. In other words, yeast aging might reflect the activity of a death pathway that normally functions in pathogen control. It might represent a fungal version the inflammatory or auto-immune response in metazoans. Therefore, it will be interesting to investigate whether exogenous or non-chromosomal DNA, such as that of viruses, also triggers the displacement of the nuclear basket from NPCs in yeast and other systems, and whether this contributes to either or both of anti-viral defence and aging. If so, aging might have emerged as an anti-viral defence.

Author Contributions:

Conceptualization: MM, ACM, YB Investigation: MM, JM, ACM Formal Analysis: MM,JM, ACM,CD Writing-original draft: YB,MM Writing – review & editing: MM,JM,JP,SAE,YB Resources: JP,SSL Supervision: YB Funding acquisition: YB

Acknowledgments:

We acknowledge Dr.Dan Jarosz, Dr. Gabriel Neurohr, Dr. Madhav Jagannathan, Dr. Patrick Meraldi ,Dr Anna Marzelliusardottir for critical reading and suggestions on the Manuscript. We acknowledge the ScopeM facility at the Institute of Biochemistry, ETH for their technical assistance. We acknowledge Elisa Dultz for providing the Chromosome II strain with the POA1::TetO array.

Funding:

YB: grant 31003A-105904 from the Swiss National Science Foundation (SNSF)

MM: ETH postdoctoral fellowship 19-1 FEL-10

JP: CIHR (Canadian institute of health research) 201809PJT-407549-BMB-CFDA-53473.

SSL: Scope M facility of ETH Zurich, Institute of Biochemistry

SAE: CIHR (Canadian institute of health research) 201809PJT-407549-BMB-CFDA-53473.

Declaration of interests:

Authors declare that they have no competing interests.

Data and materials availability:

All the raw data generated in the manuscript will be deposited in the Mendelay online repository.

Main Figure Legends

Figure 1 Old cells lose chromosomes

A) Cells carrying labeled chromosome II (Chr II) and imaged at different ages on the microfluidic chip. Time of acquisition is indicated on the left. Fluorescent markers are indicated on top. Replicative age of imaged cells (completed budding event – CBE) is indicated in merged images. Scale bar (upper right panel) is 5µm. Green arrow marks the TetR-GFP foci **B)** Schematic representation of the chromosome and minichromosome labels used in this study. **C)** Chromosome loss frequency of indicated chromosomes after 0h (~0-3 CBE) and 24h (~18-22 CBE) of imaging. The mode of chromosome visualization is indicated in parenthesis, i.e., TetR-GFP (green), TetR-mCherry (red) or mini-

547 chromosome encoded GFP (GFP exp). Chromosome loss is defined as the absence of the label in the
548 mother cell in G1 shortly after the final cell cycle, or the final anaphase. Each data point represents
549 frequency of chromosome loss in a cohort of ~50 cells. Unpaired T-test (*<0.05, **<0.005, ***<0.0005).
550
551 **Figure 2 Old cells lose chromosomes by asymmetric sister chromatid partitioning**
552 **A)** Images of anaphase cells carrying the labeled chromosome II as in Fig. 1A. Red arrows mark the old
553 SPBs. **B)** Frequency of anaphase mis-segregation events where chromosomes are visible only in the
554 mother or daughter cell (n>150) Bars are labelled as in Fig 1C. Each data point represents frequency of
555 anaphase mis-segregation in the cohort of ~50 anaphases **C**) Fraction of anaphase mis-segregation
556 events that lead to TetR-GFP foci being present only in mother or daughter cell (n=66, cohorts of 10).
557 **D)** Graphical schematic of all observed anaphase mis-segregation events and their frequency.
558 **E)** Fraction of anaphase mis-segregation events biased towards the old (red) or new SPB (pink) for mini-
559 chromosome (n=30) and Chr II with normal (Daughter(D)) and inverted segregation of the old SPB
560 (Mother (M)) (n=60 and 30). Cohorts of 10-20 missegregating anaphases **F)** Frequency of chromosome
561 II loss in *wt*, *lpl1-321*, at 0h (~0-3 CBE), 12h (~8-12 CBE) and 24h (~18-22 CBE) at 27°C. Each data
562 point represents loss frequency in a cohort of ~50 cells. Unpaired T-test (*<0.05, **<0.005, ***<0.0005).
563
564 **Figure 3 ERC formation and NPC remodeling drive chromosome loss and aging**
565 **A)** Chromosome II loss frequency per CBE in strains of indicated genotype (divided into categories of
566 5xCBE)*(N, n(cells/divisions) wt=458/8600, sir2Δ=158/1779, fob1Δ=127/2681, sgf73Δ=142/3950*
567 *mlp1Δ=302/4270).*Loss frequencies in the same age category are compared to wt. Unpaired T-test
568 (*<0.05, **<0.005, ***<0.0005). **B)** Replicative lifespan of listed genotypes (n>120 cells, Log-rank
569 (Mentel Cox) test *<0.05, **<0.005, ***<0.0005).
570
571 **Figure 4 Introns drive asymmetric chromatid partitioning and chromosome loss in aging**
572 **A)** A list of genes encoding kinetochore-associated proteins adapted from *Biggins et al 2013*. Intron
573 containing genes are marked in red. **B)** Chromosome II loss frequency at indicated aging time (top) in
574 cells of indicated genotype. *3xΔi stands for GLC7-Δi MCM21-Δi NBL1-Δi* triple mutant. Each data point
575 represents the frequency of chromosome loss in a cohort of ~50 cells. Unpaired T-test (*<0.05, **<0.005,
576 ***<0.0005). **C)** Frequency of anaphase mis-segregation of chromosome II at indicated aging time (top)
577 in cells of indicated genotype. *3xΔi stands for GLC7-Δi MCM21-Δi NBL1-Δi* triple mutant. Each data
578 point represents mis-segregation frequency in a cohort of ~50 anaphases. Loss frequencies in the same
579 age category are compared to wt. Unpaired T-test (*<0.05, **<0.005, ***<0.0005). **D)** Replicative lifespan
580 upon intron removal (n>200 cells, Log-rank (Mentel Cox) test, *<0.05, **<0.005, ***<0.0005).

581 **Figure 5 Basket displacement causes intron-dependent chromosome loss in young and old cells**
582 **A)** Stills of symmetric and asymmetric anaphases in young cells. Arrow marks the old SPB. Scale bar
583 (upper right panel) is 5µm **B)** Frequency of anaphase mis-segregation of chromosome II in cells of
584 indicated genotypes *(n>2500 cells).* Each data point represents anaphase mis-segregation frequency
585 in a cohort of >300 cells. **C)** Fraction of chromosome II mis-segregation with old (red) or new SPB (pink)
586 in anaphase cells of indicated genotype (n=30 cohorts of ~10 mis-segregation events) Unpaired T-test
587 (*<0.05, **<0.005, ***<0.0005) **D)** Chromosome II loss frequency in indicated genotype as a function of
588 CBE (categories of 5xCBE) *(N, n(cells/divisions) wt=458/8600, mlp1Δ=302/4270,3xΔi=469/9974 mlp1Δ*
589 *3xΔi=295/4757)* **E)** Replicative lifespan of listed genotypes. Red and green stars represent *p-values*
590 between the wt and the corresponding genotype. Black stars represent the p-value between *mlp1Δ* and
591 *mlp1Δ 3xΔi* (n>300 cells, Log-rank (Mentel Cox) test, *<0.05, **<0.005, ***<0.0005).
592
593 **Figure 6 Non-centromeric DNA is sufficient to drive aging and chromosome loss**
594 **A)** Schematic of transformation of chromosome II reporter strains with YRp17 (-*CEN* plasmid) and the
595 accumulation of non-centromeric plasmids. **B)** Replicative lifespan of strains with and without YRp17
596 plasmid. Red stars represent *p-value* between the YRp17 and YRp17 *3xΔi* strain. Orange stars
597 represent the *p-value* between YRp17 *3xΔi* and wt (n>200 cells, Log-rank (Mentel Cox) test, *<0.05,
598 **<0.005, ***<0.0005) **C)** Chromosome II loss frequency in indicated genotypes as a function of CBE
599 (divided into categories of 5xCBE) *(N, n(cells/divisions) wt=458/8600,3xΔi=469/9974,*+YRp17
600 *=199,2097,* + YRp17 *3xΔi=200,3134).* **D)** Replicative lifespan of *sir2Δ and sir2Δ3xΔi* strain. Stars
601 represent *p-value* between *sir2Δ and sir2Δ3xΔi* (n>200 cells, Log-rank (Mentel Cox) test, *<0.05,
602 **<0.005, ***<0.0005). **E)** Chromosome II loss frequency in indicated genotype as a function of CBE

(divided into categories of 5xCBE) *(N, n(cells/divisions) wt=458/8600,3xΔi=469/9974, sir2Δ=351,3500, sir2Δ3xΔi=350,3840).*

Figure 7 Pre-mRNA leaks to the cytoplasm of old cells
A) Images of RNA FISH targeting three long introns (*GLC7, YRA1, DBP2*) in young and old cells. **B)** Quantification of *GLC7* intron RNA FISH foci localization in young and old cells (n=295, cohorts of ~100 cells) **C)** Principle of the pre-mRNA translation reporter (left panel) adapted from (*Sorenson et al. 2014*). **D)** Images of the pre-mRNA translation reporter in cells (right panel) of indicated genotype (top) at indicated ages (bottom). **E)** Ratio of mCherry/GFP signal in the same cells at 0h and after 24 hours of aging. 119/146 cells have a ratio greater than "1" **F)** Log2 ratio of mCherry/GFP in cells of indicated genotype as a function of age, normalized to wt median at 0h (n=60, 35, 32). Unpaired T-test comparing mCherry/GFP intensity of cells at 12 or 24h (*<0.05, **<0.005, ***<0.0005).

Figure 8 Pre-mRNA leakage is sufficient to drive asymmetric chromatid partitioning
A) Chromosome II mis-segregation in cells of indicated genotypes *(n=2774,3000,5269,2650,1607).* Each data point represents anaphase mis-segregation frequency in the cohort of >300 cells **B)** Fraction of chromosome II mis-segregation with old (red) or new SPB (pink) in anaphase cells of indicated genotype (n=50,30 cohorts of ~10 mis-segregation events). Unpaired T-test (*<0.05, **<0.005, ***<0.0005).

Supplementary Figure Legends

Figure S1 Introns affect chromosome loss, but not whole nuclei mis-segregation in aging
A) Stills of a whole nuclear mis-segregation event, with both SPBs ending up in the daughter cell. **B)** Quantification of the frequency of whole nuclear mis-segregation events in wt and 3xΔ*i (*n=450 cells, cohorts of 50 cells, Unpaired T-test. **C)** Replicative lifespan of wt, *GLC7Δi, lpl1-321* and *lpl1-321 GLC7Δi* cells grown at 27 Celsius (n=300), Log-rank (Mentel Cox) test *<0.05,**<0.005,***<0.0005.**D)** Frequency of chromosome II loss in wt, *lpl1-321*, *lpl1-321 3xΔi (GLC7-Δi MCM21-Δi NBL1Δi)* at 0h (~0-3 CBE), 12h (~8-12 CBE) and 24h (~18-22 CBE) at 27°C. Each data point represents loss frequency in a cohort of ~50 cells**.** Unpaired T-test (*<0.05, **<0.005).

Figure S2 The effect of introns on chromosome loss is not chromosome-specific
A) Replicative lifespan of *wt, mad1Δ, mad2Δ* cells. n>100 cells, Log-rank (Mentel Cox) test. **B)** Frequency of chromosome II, IV and GFP minichromosome loss (See Fig 1B) in wt and upon removal of intron of *GLC7* at 24h (~18-22 CBE). Each data point represents a fraction of loss in a cohort of ~50 cells. Unpaired T-test (*<0.05, **<0.005, ***<0.0005).

Figure S3 The 3x*Δi* removal does not alter mitotic timing, growth or budding in old age due to *GLC7Δi* duplication.

A) Stills depicting the method of mitotic timing quantification in young cells, measuring the time between SPB alignment and SPB separation, marking anaphase onset **B)** Mitotic timing in wt and *3xΔi* cells (n>50, unpaired T-test). **C)** 10-fold serial dilution spot assay for different intron removal strains. YPD, two days of growth, 30°C. **D)** Measuring the timing between the emergence of the bud and cytokinesis in the final completed division of the replicative lifespan in wt and *3xΔi* cells(n>50, unpaired T-test). **E)** Map of the *GLC7* locus on chromosome V, the flanking Ty1 elements, and the result of Ty1 transposition. **F)** The result of tagging the duplicated locus with C-terminal ye-GFP tag. Upon tagging the *GLC7-Δi* but not the wt *GLC7* locus, the locus duplication becomes evident.

Figure S4 smRNA FISH probes are intron specific
A) Images of smRNA FISH experiments in wt and *GLC7-Δi* cells. **B)** Quantification of smRNA FISH foci per cell in wt and *GLC7-Δi* cells. **C)** Quantification of smRNA FISH foci per cell in wt cells at 0 and 28h of aging (n>300, cohorts of 100+ cells).

Materials and methods

Lead contact

Further information and requests for resources and reagents should be directed to and will be fulfilled by the Lead Contact, Yves Barral (yves.barral@bc.biol.ethz.ch).

654 **Materials availability**

655 This study generated ~50 novel yeast strains, derived either by crossing or transformation. All strains,
656 primers and RNA FISH probes are listed in Supplementary table 1. All resources are available to the
657 public upon request. All the raw data used in this manuscript is available in Supplementary file 1.
658
659 **Experimental Model Details**

660 **Strains**

661 All yeast strains and plasmids used in this study are listed in the **Supplementary table 1**. Strains are
662 derived from S288C background. For every strain derived from a cross, an appropriate control strain
663 was always selected from the same tetrad. Protein C-terminal yeGFP-tag and knock-out strains were
664 generated using methods described in *Janke et al 2004* [69]. All cultures were grown using standard
665 conditions at 160 rpm, in YPD or synthetic drop-out medium supplemented with 0.1% BSA for aging
666 chips (SD-medium; ForMedium, Norfolk, UK) at 25°C or 30°C.

667 **Intron-less strains**
668
669 Intron deletions were conducted in two independent colonies of the strain JPY10I, as outlined previously
670 in Parenteau *et al* 2008 [40]. Briefly, each intron was individually deleted using a modified two-step process
671 (pop-in / pop-out), ensuring the absence of any additional sequence or markers post-deletion. The
672 deletions were done in diploid strains, confirmed via PCR, and three distinct haploid strains bearing the
673 confirmed deletions were chosen for subsequent analyses. Combinations of different Δ-intron strains
674 have been derived by crossing and validated by PCR for the absence of the intron.
675
676 **Chromosome and Plasmid reporter strains**
677
678 Multiple chromosomes and minichromosome visualization strains have been used in this study: **1)**
679 Chromosome II reporter strain, with the centromere proximal TetO array (*POA1* locus) strain was kindly
680 provided by Elisa Dultz from the Weis Lab, ETH, institute of Biochemistry (internal reference KWY3759).
681 **2)** Chromosome IV TetO (Centromere proximal) and LacO (centromere distal) were acquired from
682 strains used in *Neurohr et al 2011* [17], originally derived from *Vas AC et al 2006* [70] **3)** Ubi-GFP
683 minichromosome (PYB 2665) was derived by cloning UBIYdkGFP* from *Houser et al 2012* (PNC 1136)
684 [71] into a PYB 2640 backbone by homologous recombination in yeast. **4)** A minichromosome reporter
685 containing the TetO array was previously described in *Denoth-Lippuner et al 2014* [12].

686 **Plasmids:**

687 For the assessment of centromeric plasmid loss using the TeO-TetR-GFP system, we used the plasmid
688 already published in *Dennoth-Lipptuner et al 2014*[12]. For construction of centromeric plasmid encoding
689 GFP as a reporter, we used a short-lived GFP (UBIYΔkGFP*–SpHis5–TIM9 in pUC118) available from
690 Addgene(pNC1136). Ubi-GFP was amplified from PNC1136 with primers MM 311/312 (listed in
691 Supplementary table1). The resulting PCR product contained 50 bp homologous overhangs to another
692 plasmid containing a centromere, pADH1 promoter and a pUG23 backbone (PYB2640). The template
693 plasmid (PYB2640) was digested with MscI and Sac II and co-transformed with amplified UBIYΔkGFP*
694 PCR product to yeast to assemble the plasmid with *CEN* and pADH1-UBIYΔkGFP* via homologous
695 recombination. Successful recombinants were then selected on *-LEU* media after transformation.
696 Recombinant plasmid was extracted from yeast and transformed into bacteria. The correct plasmid
697 assembly was validated by sequencing. A full sequence of the assembled plasmid is available in
698 supplementary data. For transformation of yeast with a non-centromeric plasmid, we have utilized Yeast
699 Replicative Plasmid 17(YRp17) from *Mann et al 1983*. The full sequence of YRp17 is available online
700 and in the supplementary data.

701 **Materials and methods**
702
703 **Microscopy**

704 For confocal fluorescent microscopy, yeast cells were precultured in YPD and then washed in synthetic
705 drop-out medium. One ml of cells from exponential growing cultures with OD <1 was concentrated by

706 centrifugation at 1500 rcf, washed in SD complete, and resuspended in ~10 µl of low fluorescent SD-
707 medium, spotted on a round coverslip and immobilized with a SD/agar patch. The cells were imaged in
708 >15 z-stacks slices with 0.3 µm spacing, with a 100×/1.4 NA objective on a DeltaVision microscope
709 (Applied Precision) equipped with a CCD HQ2 camera (Roper), 250 W Xenon lamps, Softworx software
710 (Applied Precision) and a temperature chamber set to 30°C.
711
712 **Aging microfluidic platform**

713 Chromosome segregation and protein intensity during aging were assessed using the high-throughput
714 yeast aging analysis (HYAA) microfluidics dissection platform [19]. The PDMS (polydimethylsiloxane)
715 microchannel is made by soft-lithography and bonded on the 30 mm micro-well cover glass in the 55
716 mm glass bottom dish (Cellvis, CA, USA). For lifespan analyses, a chip with a new cell trapping design
717 was used [5], to ensure excellent retention of old cells.

718 To start the aging experiment, yeast cells were pre-cultured for 24 hr in SD-full media supplemented
719 with 0.1% Albumin Bovine Serum (protease free BSA; Acros Organics, Geel, Belgium). Young cells from
720 an exponentially growing culture were captured in the traps of the microfluidic chip; the chip was
721 continuously flushed with fresh medium at a constant flow of 10 µl/min, using a Harvard PHD Ultra
722 syringe pump (Harvard Apparatus, Holiston, MA, USA) with 60 ml syringe per lane, with inner diameter
723 26.7 mm (Becton Dickinson, Franklin Lakes, NJ, USA). Bright field images in a single z focal plane were
724 recorded every 15 min throughout the duration of the entire experiment to measure replicative age of
725 cells. To record fluorescent signals, images with a florescent lamp and at least 13x z-stacks (0.5 µm
726 step) were acquired in 12h intervals. For imaging we used an epi-fluorescent microscope (TiE, Nikon
727 Instruments, Tokyo, Japan) controlled by Micro-Manager 1.4.23 software [72], with a Plan Apo 60 × 1.4
728 NA objective. For fluorescence illumination of the GFP and mCherry labelled proteins, a Lumencor
729 Spectra-X LED Light Engine was used. Z stacks of >13 slices with 0.5 µm spacing were recorded for
730 fluorescent imaging every 12 hours to cover the entire volume of the nucleus during the aging process.
731 Transmitted light imaging was done in a single Z plane to minimize the light exposure of the cells. The
732 age of the cell was defined by the number of daughter cells that emerged during the budding cycles
733 (CBE).

734 **Chromosome loss assessment**

735 For the assessment of chromosome and mini-chromosome loss and mis-segregation in aging, trapped
736 cells in the chip that had the labeled chromosomes at the initial time point of 0h (~virtually all cells) were
737 followed in transmitted light channel and fluorescent images were acquired every 12 hours. Only cells
738 where the entire volume of the nucleus was in focus and imaged, and where SPB was clearly visible
739 were considered in the analysis. The background fluorescence was subtracted in FIJI using a subtract
740 background function. The aged nuclei were examined by scrolling through the z stack (>13 stacks,
741 0,5um step) in both channels, to validate the presence of the SPBs and TetR foci in the mother or the
742 daughter cell. "Chromosome loss" refers to two quantified events: 1) The absence of the chromosome
743 from a mother or a daughter cell compartment during anaphase 2) A G1 mother cell that just underwent
744 its final division and is clearly viable, with a present SPB dot, but no chromosome dot. When
745 "Chromosome loss" is listed, it pertains to the sum of these two events. When "chromosome loss in
746 anaphase" is listed, it only pertains to the loss frequency observed during anaphase. Cells which lost
747 chromosomes due to abnormal mitotic events in the last replicative division, such as SPB
748 overamplification or full nuclei migration into the bud (Combined ~10% of all cells in the final replicative
749 division) were discarded from the quantifications. All cells were examined in the DIC channel for signs
750 of disrupted morphology indicating cell death and followed up in DIC to confirm cell death after
751 chromosome loss. For the assessment of minichromosome loss in aging (TetO array or ubi-GFP
752 minichromosome) the yeast cultures were grown in SD-LEU or SD-URA selective media enabling
753 minichromosome maintenance in all starting young cells. When loaded onto an aging chip cell were
754 transferred to SD complete media, allowing them to lose the minichromosome during aging without
755 inducing cell death. As the cells were grown in selective media, the minichromosome loss rate at 0h is
756 N/A. In general, aging chips are not suitable for measurement of chromosome loss frequency in young
757 cells, as cells within the young population that are missegregating chromosomes are usually stressed
758 and enlarged, and thus cannot be loaded into the microfluidic traps intended for normal young cells. For
759 chromosome mis-segregation frequency in young cells, we have used classical confocal imaging on a
760 patch of SD agar, as described in the Microscopy section.

761 **Measurements of chromosome loss per CBE**
762
763 To measure chromosome loss probability per Completed Budding Event (CBE), we utilized at least 150
764 cells per genotype and quantified the number of cells that lost the reporter chromosome during a specific
765 replicative division. The number of losses at a specific CBE was then divided by total number of cells
766 which passed through mitosis at that CBE number to give the probability of chromosome loss per CBE.
767 Categories of 5x CBE and its mean value of chromosome loss were plotted along with its SEM.
768
769 **Mother Enrichment Program (MEP) with FACS and RNA FISH**
770
771 Mother Enrichment Program was performed according to the standard procedure, using the strains
772 acquired from the Gotchling Lab [43]. Cells were labeled with Biotin and aged for 28h, after which they
773 were fixed in 4% PFA for 30 minutes. The cells were then stained with streptavidin conjugated with a
774 FACS compatible fluorophore (647nm) and sorted using FACSAria III at the Flow Cytometry Core
775 Facility at ETH Zurich to enrich for old mother cells. After FACS sorting, single molecule RNA FISH with
776 Stellaris® probes designed for introns of *GLC7, YRA1, DBP2* was performed as described in *Rahman*
777 *et al 2013* [73].
778
779 **Quantification and Statistical analysis.**
780
781 Statistical analyses were performed using GraphPad Prism 10 software

782 **Resources table**

REAGENT or RESOURCE	SOURCE	Reference
Critical commercial assays		
GEL extraction	QIAGEN	Ref:28604
Plasmid extraction	MACHEREY-NAGEL	Ref:740588.250
Deposited data		
Raw data from this study	Mihailo Mirkovic	Supp table 2
Experimental models: Organisms/strains		
Full strain list	Mihailo Mirkovic	Supp table 1
Primers	Mihailo Mirkovic	See Sup. Table 1
smRNA FISH probes	Biosearch Technologies	See Sup. Table 1
Recombinant DNA		Internal reference
CEN TetO-plasmid	*Dennoth-L et al 2014*	YYB 16094
CEN Ubi-GFP plasmid	This study	PYB 2665
YRp17 plasmid	*Mann C et al 1983*	PYB 546
Software and algorithms		
Graphpad Prism	Dotmatics	
ImageJ-FIJI		
Microsoft Excel	Microsoft	
Microsoft Word	Microsoft	
Adobe Illustrator	Adobe	

783

784

785 **References**

786 1. Denoth Lippuner, A., Julou, T., and Barral, Y. (2014). Budding yeast as a model organism to
787 study the effects of age. FEMS Microbiol Rev *38*, 300-325. 10.1111/1574-6976.12060.
788 2. Lopez-Otin, C., Blasco, M.A., Partridge, L., Serrano, M., and Kroemer, G. (2023). Hallmarks of
789 aging: An expanding universe. Cell *186*, 243-278. 10.1016/j.cell.2022.11.001.

790 3. Janssens, G.E., and Veenhoff, L.M. (2016). Evidence for the hallmarks of human aging in
791 replicatively aging yeast. Microb Cell *3*, 263-274. 10.15698/mic2016.07.510.
792 4. Rempel, I.L., Steen, A., and Veenhoff, L.M. (2020). Poor old pores-The challenge of making
793 and maintaining nuclear pore complexes in aging. FEBS J *287*, 1058-1075.
794 10.1111/febs.15205.
795 5. Meinema, A.C., Marzelliusardottir, A., Mirkovic, M., Aspert, T., Lee, S.S., Charvin, G., and
796 Barral, Y. (2022). DNA circles promote yeast ageing in part through stimulating the
797 reorganization of nuclear pore complexes. Elife *11*. 10.7554/eLife.71196.
798 6. Rempel, I.L., Crane, M.M., Thaller, D.J., Mishra, A., Jansen, D.P., Janssens, G., Popken, P.,
799 Aksit, A., Kaeberlein, M., van der Giessen, E., et al. (2019). Age-dependent deterioration of
800 nuclear pore assembly in mitotic cells decreases transport dynamics. Elife *8*.
801 10.7554/eLife.48186.
802 7. Sinclair, D.A., and Guarente, L. (1997). Extrachromosomal rDNA circles--a cause of aging in
803 yeast. Cell *91*, 1033-1042. 10.1016/s0092-8674(00)80493-6.
804 8. Jin, M., Li, Y., O'Laughlin, R., Bittihn, P., Pillus, L., Tsimring, L.S., Hasty, J., and Hao, N. (2019).
805 Divergent Aging of Isogenic Yeast Cells Revealed through Single-Cell Phenotypic Dynamics.
806 Cell Syst *8*, 242-253 e243. 10.1016/j.cels.2019.02.002.
807 9. Morlot, S., Song, J., Leger-Silvestre, I., Matifas, A., Gadal, O., and Charvin, G. (2019). Excessive
808 rDNA Transcription Drives the Disruption in Nuclear Homeostasis during Entry into
809 Senescence in Budding Yeast. Cell Rep *28*, 408-422 e404. 10.1016/j.celrep.2019.06.032.
810 10. Moller, H.D., Mohiyuddin, M., Prada-Luengo, I., Sailani, M.R., Halling, J.F., Plomgaard, P.,
811 Maretty, L., Hansen, A.J., Snyder, M.P., Pilegaard, H., et al. (2018). Circular DNA elements of
812 chromosomal origin are common in healthy human somatic tissue. Nat Commun *9*, 1069.
813 10.1038/s41467-018-03369-8.
814 11. Bitterman, K.J., Medvedik, O., and Sinclair, D.A. (2003). Longevity regulation in
815 Saccharomyces cerevisiae: linking metabolism, genome stability, and heterochromatin.
816 Microbiol Mol Biol Rev *67*, 376-399, table of contents. 10.1128/MMBR.67.3.376-399.2003.
817 12. Denoth-Lippuner, A., Krzyzanowski, M.K., Stober, C., and Barral, Y. (2014). Role of SAGA in
818 the asymmetric segregation of DNA circles during yeast ageing. Elife *3*. 10.7554/eLife.03790.
819 13. Shcheprova, Z., Baldi, S., Frei, S.B., Gonnet, G., and Barral, Y. (2008). A mechanism for
820 asymmetric segregation of age during yeast budding. Nature *454*, 728-734.
821 10.1038/nature07212.
822 14. Baldi, S., Bolognesi, A., Meinema, A.C., and Barral, Y. (2017). Heat stress promotes longevity
823 in budding yeast by relaxing the confinement of age-promoting factors in the mother cell.
824 Elife *6*. 10.7554/eLife.28329.
825 15. Boveri, T. (2008). Concerning the origin of malignant tumours by Theodor Boveri. Translated
826 and annotated by Henry Harris. J Cell Sci *121 Suppl 1*, 1-84. 10.1242/jcs.025742.
827 16. Jacobs, P.A., Court Brown, W.M., and Doll, R. (1961). Distribution of human chromosome
828 counts in relation to age. Nature *191*, 1178-1180. 10.1038/1911178a0.
829 17. Neurohr, G., Naegeli, A., Titos, I., Theler, D., Greber, B., Diez, J., Gabaldon, T., Mendoza, M.,
830 and Barral, Y. (2011). A midzone-based ruler adjusts chromosome compaction to anaphase
831 spindle length. Science *332*, 465-468. 10.1126/science.1201578.
832 18. Kruitwagen, T., Chymkowitch, P., Denoth-Lippuner, A., Enserink, J., and Barral, Y. (2018).
833 Centromeres License the Mitotic Condensation of Yeast Chromosome Arms. Cell *175*, 780-
834 795 e715. 10.1016/j.cell.2018.09.012.
835 19. Jo, M.C., Liu, W., Gu, L., Dang, W., and Qin, L. (2015). High-throughput analysis of yeast
836 replicative aging using a microfluidic system. Proc Natl Acad Sci U S A *112*, 9364-9369.
837 10.1073/pnas.1510328112.
838 20. Crane, M.M., Russell, A.E., Schafer, B.J., Blue, B.W., Whalen, R., Almazan, J., Hong, M.G.,
839 Nguyen, B., Goings, J.E., Chen, K.L., et al. (2019). DNA damage checkpoint activation impairs
840 chromatin homeostasis and promotes mitotic catastrophe during aging. Elife *8*.
841 10.7554/eLife.50778.

842 21. Lengefeld, J., Hotz, M., Rollins, M., Baetz, K., and Barral, Y. (2017). Budding yeast Wee1
843 distinguishes spindle pole bodies to guide their pattern of age-dependent segregation. Nat
844 Cell Biol *19*, 941-951. 10.1038/ncb3576.
845 22. Pereira, G., Tanaka, T.U., Nasmyth, K., and Schiebel, E. (2001). Modes of spindle pole body
846 inheritance and segregation of the Bfa1p-Bub2p checkpoint protein complex. EMBO J *20*,
847 6359-6370. 10.1093/emboj/20.22.6359.
848 23. Hotz, M., Leisner, C., Chen, D., Manatschal, C., Wegleiter, T., Ouellet, J., Lindstrom, D.,
849 Gottschling, D.E., Vogel, J., and Barral, Y. (2012). Spindle pole bodies exploit the mitotic exit
850 network in metaphase to drive their age-dependent segregation. Cell *148*, 958-972.
851 10.1016/j.cell.2012.01.041.
852 24. Biggins, S., Severin, F.F., Bhalla, N., Sassoon, I., Hyman, A.A., and Murray, A.W. (1999). The
853 conserved protein kinase Ipl1 regulates microtubule binding to kinetochores in budding
854 yeast. Genes Dev *13*, 532-544. 10.1101/gad.13.5.532.
855 25. Cheeseman, I.M., Anderson, S., Jwa, M., Green, E.M., Kang, J., Yates, J.R., 3rd, Chan, C.S.,
856 Drubin, D.G., and Barnes, G. (2002). Phospho-regulation of kinetochore-microtubule
857 attachments by the Aurora kinase Ipl1p. Cell *111*, 163-172. 10.1016/s0092-8674(02)00973-x.
858 26. Tanaka, T.U., Rachidi, N., Janke, C., Pereira, G., Galova, M., Schiebel, E., Stark, M.J., and
859 Nasmyth, K. (2002). Evidence that the Ipl1-Sli15 (Aurora kinase-INCENP) complex promotes
860 chromosome bi-orientation by altering kinetochore-spindle pole connections. Cell *108*, 317-
861 329. 10.1016/s0092-8674(02)00633-5.
862 27. Kaeberlein, M., McVey, M., and Guarente, L. (1999). The SIR2/3/4 complex and SIR2 alone
863 promote longevity in Saccharomyces cerevisiae by two different mechanisms. Genes Dev *13*,
864 2570-2580. 10.1101/gad.13.19.2570.
865 28. Defossez, P.A., Prusty, R., Kaeberlein, M., Lin, S.J., Ferrigno, P., Silver, P.A., Keil, R.L., and
866 Guarente, L. (1999). Elimination of replication block protein Fob1 extends the life span of
867 yeast mother cells. Mol Cell *3*, 447-455. 10.1016/s1097-2765(00)80472-4.
868 29. De Magistris, P. (2021). The Great Escape: mRNA Export through the Nuclear Pore Complex.
869 Int J Mol Sci *22*. 10.3390/ijms222111767.
870 30. Niepel, M., Molloy, K.R., Williams, R., Farr, J.C., Meinema, A.C., Vecchietti, N., Cristea, I.M.,
871 Chait, B.T., Rout, M.P., and Strambio-De-Castillia, C. (2013). The nuclear basket proteins
872 Mlp1p and Mlp2p are part of a dynamic interactome including Esc1p and the proteasome.
873 Mol Biol Cell *24*, 3920-3938. 10.1091/mbc.E13-07-0412.
874 31. Raices, M., and D'Angelo, M.A. (2017). Nuclear pore complexes and regulation of gene
875 expression. Curr Opin Cell Biol *46*, 26-32. 10.1016/j.ceb.2016.12.006.
876 32. Galy, V., Gadal, O., Fromont-Racine, M., Romano, A., Jacquier, A., and Nehrbass, U. (2004).
877 Nuclear retention of unspliced mRNAs in yeast is mediated by perinuclear Mlp1. Cell *116*, 63-
878 73. 10.1016/s0092-8674(03)01026-2.
879 33. Bonnet, A., and Palancade, B. (2015). Intron or no intron: a matter for nuclear pore
880 complexes. Nucleus *6*, 455-461. 10.1080/19491034.2015.1116660.
881 34. Iouk, T., Kerscher, O., Scott, R.J., Basrai, M.A., and Wozniak, R.W. (2002). The yeast nuclear
882 pore complex functionally interacts with components of the spindle assembly checkpoint. J
883 Cell Biol *159*, 807-819. 10.1083/jcb.200205068.
884 35. Scott, R.J., Lusk, C.P., Dilworth, D.J., Aitchison, J.D., and Wozniak, R.W. (2005). Interactions
885 between Mad1p and the nuclear transport machinery in the yeast. Molecular Biology of the
886 Cell *16*, 4362-4374. 10.1091/mbc.E05-01-0011.
887 36. Pinsky, B.A., Kotwaliwale, C.V., Tatsutani, S.Y., Breed, C.A., and Biggins, S. (2006).
888 Glc7/protein phosphatase 1 regulatory subunits can oppose the Ipl1/aurora protein kinase by
889 redistributing Glc7. Mol Cell Biol *26*, 2648-2660. 10.1128/MCB.26.7.2648-2660.2006.
890 37. Poddar, A., Roy, N., and Sinha, P. (1999). MCM21 and MCM22, two novel genes of the yeast
891 Saccharomyces cerevisiae are required for chromosome transmission. Mol Microbiol *31*, 349-
892 360. 10.1046/j.1365-2958.1999.01179.x.
893 38. Nakajima, Y., Tyers, R.G., Wong, C.C., Yates, J.R., 3rd, Drubin, D.G., and Barnes, G. (2009).
894 Nbl1p: a Borealin/Dasra/CSC-1-like protein essential for Aurora/Ipl1 complex function and

895 integrity in Saccharomyces cerevisiae. Mol Biol Cell *20*, 1772-1784. 10.1091/mbc.e08-10-
896 1011.
897 39. Parenteau, J., Maignon, L., Berthoumieux, M., Catala, M., Gagnon, V., and Abou Elela, S.
898 (2019). Introns are mediators of cell response to starvation. Nature *565*, 612-617.
899 10.1038/s41586-018-0859-7.
900 40. Parenteau, J., Durand, M., Veronneau, S., Lacombe, A.A., Morin, G., Guerin, V., Cecez, B.,
901 Gervais-Bird, J., Koh, C.S., Brunelle, D., et al. (2008). Deletion of many yeast introns reveals a
902 minority of genes that require splicing for function. Mol Biol Cell *19*, 1932-1941.
903 10.1091/mbc.e07-12-1254.
904 41. Juneau, K., Miranda, M., Hillenmeyer, M.E., Nislow, C., and Davis, R.W. (2006). Introns
905 regulate RNA and protein abundance in yeast. Genetics *174*, 511-518.
906 10.1534/genetics.106.058560.
907 42. Mann, C., and Davis, R.W. (1983). Instability of dicentric plasmids in yeast. Proc Natl Acad Sci
908 U S A *80*, 228-232. 10.1073/pnas.80.1.228.
909 43. Lindstrom, D.L., and Gottschling, D.E. (2009). The mother enrichment program: a genetic
910 system for facile replicative life span analysis in Saccharomyces cerevisiae. Genetics *183*, 413-
911 422, 411SI-413SI. 10.1534/genetics.109.106229.
912 44. Sorenson, M.R., and Stevens, S.W. (2014). Rapid identification of mRNA processing defects
913 with a novel single-cell yeast reporter. RNA *20*, 732-745. 10.1261/rna.042663.113.
914 45. Hackmann, A., Wu, H., Schneider, U.M., Meyer, K., Jung, K., and Krebber, H. (2014). Quality
915 control of spliced mRNAs requires the shuttling SR proteins Gbp2 and Hrb1. Nat Commun *5*,
916 3123. 10.1038/ncomms4123.
917 46. Hurt, E., Luo, M.J., Rother, S., Reed, R., and Strasser, K. (2004). Cotranscriptional recruitment
918 of the serine-arginine-rich (SR)-like proteins Gbp2 and Hrb1 to nascent mRNA via the TREX
919 complex. Proc Natl Acad Sci U S A *101*, 1858-1862. 10.1073/pnas.0308663100.
920 47. Windgassen, M., Sturm, D., Cajigas, I.J., Gonzalez, C.I., Seedorf, M., Bastians, H., and Krebber,
921 H. (2004). Yeast shuttling SR proteins Npl3p, Gbp2p, and Hrb1p are part of the translating
922 mRNPs, and Npl3p can function as a translational repressor. Mol Cell Biol *24*, 10479-10491.
923 10.1128/MCB.24.23.10479-10491.2004.
924 48. Stevens, S.W., and Abelson, J. (1999). Purification of the yeast U4/U6.U5 small nuclear
925 ribonucleoprotein particle and identification of its proteins. Proc Natl Acad Sci U S A *96*,
926 7226-7231. 10.1073/pnas.96.13.7226.
927 49. Murphy, M.W., Olson, B.L., and Siliciano, P.G. (2004). The yeast splicing factor Prp40p
928 contains functional leucine-rich nuclear export signals that are essential for splicing. Genetics
929 *166*, 53-65. 10.1534/genetics.166.1.53.
930 50. Haber, J.E. (2012). Mating-type genes and MAT switching in Saccharomyces cerevisiae.
931 Genetics *191*, 33-64. 10.1534/genetics.111.134577.
932 51. Rine, J., and Herskowitz, I. (1987). Four genes responsible for a position effect on expression
933 from HML and HMR in Saccharomyces cerevisiae. Genetics *116*, 9-22.
934 10.1093/genetics/116.1.9.
935 52. Gottschling, D.E., Aparicio, O.M., Billington, B.L., and Zakian, V.A. (1990). Position effect at S.
936 cerevisiae telomeres: reversible repression of Pol II transcription. Cell *63*, 751-762.
937 10.1016/0092-8674(90)90141-z.
938 53. Smith, J.S., and Boeke, J.D. (1997). An unusual form of transcriptional silencing in yeast
939 ribosomal DNA. Genes Dev *11*, 241-254. 10.1101/gad.11.2.241.
940 54. Kobayashi, T., Heck, D.J., Nomura, M., and Horiuchi, T. (1998). Expansion and contraction of
941 ribosomal DNA repeats in Saccharomyces cerevisiae: requirement of replication fork blocking
942 (Fob1) protein and the role of RNA polymerase I. Genes Dev *12*, 3821-3830.
943 10.1101/gad.12.24.3821.
944 55. Gomez-Montalvo, J., de Obeso Fernandez Del Valle, A., De la Cruz Gutierrez, L.F., Gonzalez-
945 Meljem, J.M., and Scheckhuber, C.Q. (2024). Replicative aging in yeast involves dynamic
946 intron retention patterns associated with mRNA processing/export and protein
947 ubiquitination. Microb Cell *11*, 69-78. 10.15698/mic2024.02.816.

948 56. Lim, C.S., Weinstein, B.N., Roy, S.W., and Brown, C.M. (2021). Analysis of Fungal Genomes
949 Reveals Commonalities of Intron Gain or Loss and Functions in Intron-Poor Species. Mol Biol
950 Evol *38*, 4166-4186. 10.1093/molbev/msab094.
951 57. Carmody, S.R., Tran, E.J., Apponi, L.H., Corbett, A.H., and Wente, S.R. (2010). The mitogen-
952 activated protein kinase Slt2 regulates nuclear retention of non-heat shock mRNAs during
953 heat shock-induced stress. Mol Cell Biol *30*, 5168-5179. 10.1128/MCB.00735-10.
954 58. Yona, A.H., Manor, Y.S., Herbst, R.H., Romano, G.H., Mitchell, A., Kupiec, M., Pilpel, Y., and
955 Dahan, O. (2012). Chromosomal duplication is a transient evolutionary solution to stress.
956 Proc Natl Acad Sci U S A *109*, 21010-21015. 10.1073/pnas.1211150109.
957 59. Chen, G., Bradford, W.D., Seidel, C.W., and Li, R. (2012). Hsp90 stress potentiates rapid
958 cellular adaptation through induction of aneuploidy. Nature *482*, 246-250.
959 10.1038/nature10795.
960 60. Shen, L., Wang, Y.T., Tang, X.X., Zhang, K., Wang, P.M., Sui, Y., and Zheng, D.Q. (2020). Heat
961 shock drives genomic instability and phenotypic variations in yeast. AMB Express *10*, 146.
962 10.1186/s13568-020-01091-7.
963 61. Gilchrist, C., and Stelkens, R. (2019). Aneuploidy in yeast: Segregation error or adaptation
964 mechanism? Yeast *36*, 525-539. 10.1002/yea.3427.
965 62. Ori, A., Toyama, B.H., Harris, M.S., Bock, T., Iskar, M., Bork, P., Ingolia, N.T., Hetzer, M.W.,
966 and Beck, M. (2015). Integrated Transcriptome and Proteome Analyses Reveal Organ-Specific
967 Proteome Deterioration in Old Rats. Cell Syst *1*, 224-237. 10.1016/j.cels.2015.08.012.
968 63. Malik, S.C., Lin, J.D., Ziegler-Waldkirch, S., Tholen, S., Deshpande, S.S., Schwabenland, M.,
969 Schilling, O., Vlachos, A., Meyer-Luehmann, M., and Schachtrup, C. (2023). Tpr Misregulation
970 in Hippocampal Neural Stem Cells in Mouse Models of Alzheimer's Disease. Cells *12*.
971 10.3390/cells12232757.
972 64. Mariotti, M., Kerepesi, C., Oliveros, W., Mele, M., and Gladyshev, V.N. (2022). Deterioration
973 of the human transcriptome with age due to increasing intron retention and spurious
974 splicing. bioRxiv, 2022.2003.2014.484341. 10.1101/2022.03.14.484341.
975 65. Adusumalli, S., Ngian, Z.K., Lin, W.Q., Benoukraf, T., and Ong, C.T. (2019). Increased intron
976 retention is a post-transcriptional signature associated with progressive aging and
977 Alzheimer's disease. Aging Cell *18*, e12928. 10.1111/acel.12928.
978 66. Huang, W., Kew, C., Fernandes, S.A., Lohrke, A., Han, L., Demetriades, C., and Antebi, A.
979 (2022). Decreased spliceosome fidelity and egl-8 intron retention inhibit mTORC1 signaling to
980 promote longevity. Nat Aging *2*, 796-808. 10.1038/s43587-022-00275-z.
981 67. Funk, L., Su, K.C., Ly, J., Feldman, D., Singh, A., Moodie, B., Blainey, P.C., and Cheeseman, I.M.
982 (2022). The phenotypic landscape of essential human genes. Cell *185*, 4634-4653 e4622.
983 10.1016/j.cell.2022.10.017.
984 68. Larrieu, D., Vire, E., Robson, S., Breusegem, S.Y., Kouzarides, T., and Jackson, S.P. (2018).
985 Inhibition of the acetyltransferase NAT10 normalizes progeric and aging cells by rebalancing
986 the Transportin-1 nuclear import pathway. Sci Signal *11*. 10.1126/scisignal.aar5401.
987 69. Janke, C., Magiera, M.M., Rathfelder, N., Taxis, C., Reber, S., Maekawa, H., Moreno-Borchart,
988 A., Doenges, G., Schwob, E., Schiebel, E., and Knop, M. (2004). A versatile toolbox for PCR-
989 based tagging of yeast genes: new fluorescent proteins, more markers and promoter
990 substitution cassettes. Yeast *21*, 947-962. 10.1002/yea.1142.
991 70. Vas, A.C., Andrews, C.A., Kirkland Matesky, K., and Clarke, D.J. (2007). In vivo analysis of
992 chromosome condensation in Saccharomyces cerevisiae. Mol Biol Cell *18*, 557-568.
993 10.1091/mbc.e06-05-0454.
994 71. Houser, J.R., Ford, E., Chatterjea, S.M., Maleri, S., Elston, T.C., and Errede, B. (2012). An
995 improved short-lived fluorescent protein transcriptional reporter for Saccharomyces
996 cerevisiae. Yeast *29*, 519-530. 10.1002/yea.2932.
997 72. Edelstein, A.D., Tsuchida, M.A., Amodaj, N., Pinkard, H., Vale, R.D., and Stuurman, N. (2014).
998 Advanced methods of microscope control using muManager software. J Biol Methods *1*.
999 10.14440/jbm.2014.36.

1000 73. Rahman, S., and Zenklusen, D. (2013). Single-molecule resolution fluorescent in situ
1001 hybridization (smFISH) in the yeast S. cerevisiae. Methods Mol Biol *1042*, 33-46.
1002 10.1007/978-1-62703-526-2_3.

1003

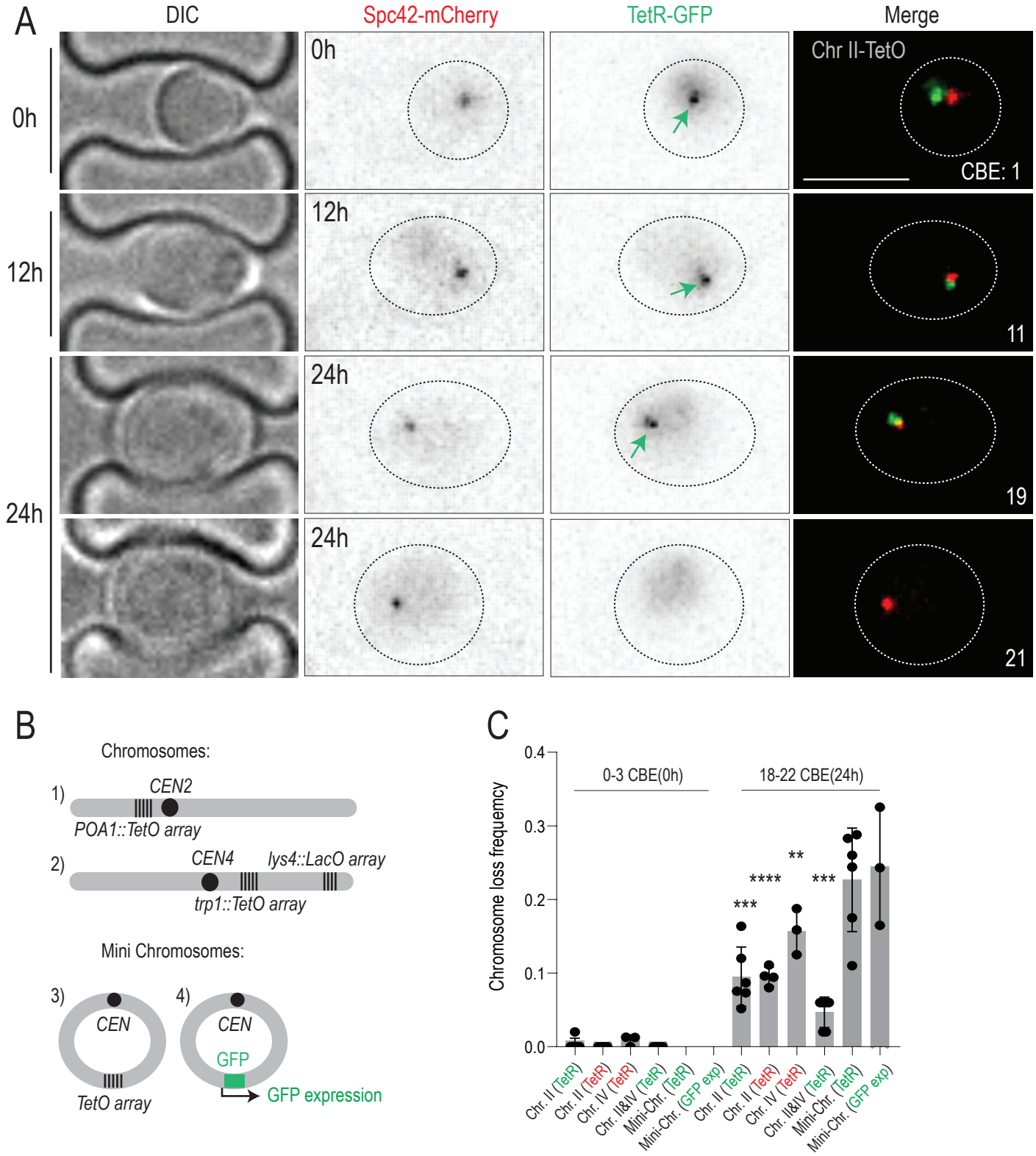
A
DIC
Spc42-mCherry
TetR-GFP
Merge
0h
12h
24h
Chr II-TetO
CBE: 1
11
19
21
B
Chromosomes:
1)
CEN2
POA1::TetO array
2)
CEN4
lys4::LacO array
trp1::TetO array
Mini Chromosomes:
3)
CEN
TetO array
4)
CEN
GFP
GFP expression
C
Chromosome loss frequency
0-3 CBE(0h)
18-22 CBE(24h)
0.0
0.1
0.2
0.3
0.4
***
****
**
***
Chr. II (TetR)
Chr. II (TetR)
Chr. IV (TetR)
Chr. II&IV (TetR)
Mini-Chr. (TetR)
Mini-Chr. (GFP exp)
Chr. II (TetR)
Chr. II (TetR)
Chr. IV (TetR)
Chr. II&IV (TetR)
Mini-Chr. (TetR)
Mini-Chr. (GFP exp)

Figure 1

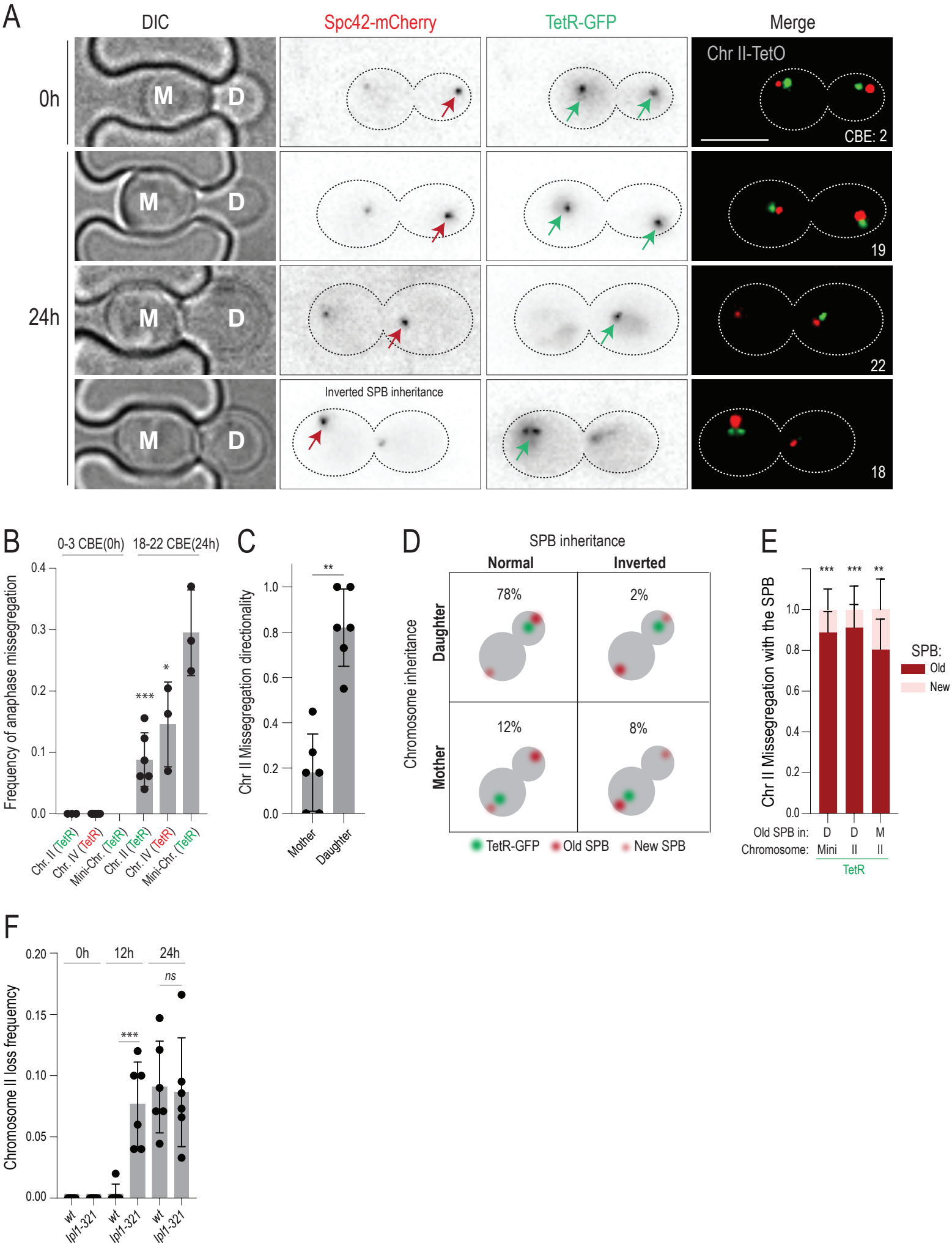
A
DIC
Spc42-mCherry
TetR-GFP
Merge
0h
24h
M
D
Chr II-TetO
CBE: 2
19
22
18
Inverted SPB inheritance
B
0-3 CBE(0h)
18-22 CBE(24h)
Frequency of anaphase missegregation
Chr. II (TetR)
Chr. IV (TetR)
Mini-Chr. (TetR)
C
Chr II Missegregation directionality
Mother
Daughter
D
SPB inheritance
Normal
Inverted
Chromosome inheritance
Daughter
Mother
78%
2%
12%
8%
TetR-GFP
Old SPB
New SPB
E
Chr II Missegregation with the SPB
SPB:
Old
New
Old SPB in:
Chromosome:
Mini
II
TetR
F
Chromosome II loss frequency
0h
12h
24h
ns
wt
lpl1-321

Figure 2

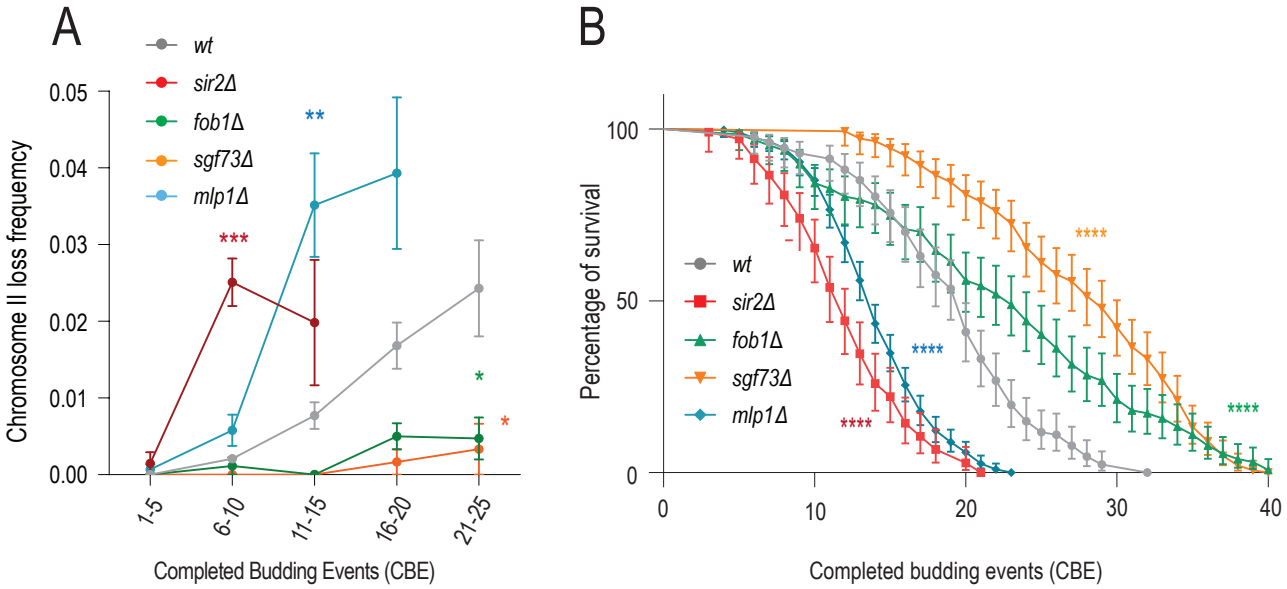
A
wt
sir2Δ
fob1Δ
sgf73Δ
mlp1Δ
Chromosome II loss frequency
0.05
0.04
0.03
0.02
0.01
0.00
***
**
*
*
1-5
6-10
11-15
16-20
21-25
Completed Budding Events (CBE)
B
Percentage of survival
100
50
0
wt
sir2Δ
fob1Δ
sgf73Δ
mlp1Δ
****
****
****
****
0
10
20
30
40
Completed budding events (CBE)

Figure 3

A

Yeast genes encoding kinetochore-associated proteins

CBF3	CCAN	CPC	SAC
NDC10	*MIF2*	*IPL1*	*MAD1*
CEP3	*CSE4*	*SLI15*	*MAD2*
CTF13	*CTF19*	*NBL1*	*BUB1*
SKP1	*OKP1*	*BIR1*	*BUB3*
	MCM21	SPC105	*MPS1*
CBF1	*AME1*	*SPC105*	Motor
	CHL4	*YDR532*	*KIP1*
MIS12	*CNN1*	DAM1	*KIP3*
MTW1	*WIP1*	*ASK1*	*CIN8*
DSN1	*MHF1*	*DAD1*	*KAR3*
NNF1	*MHF2*	*DAD2*	MAPS
NSL1	*MCM16*	*DAD3*	*SLK19*
	CTF3	*DAD4*	*BIK1*
NDC80	*MCM22*	*DAM1*	Phosphatase
NDC80	*MCM19*	*DUO1*	*GLC7*
NUF2	*NKP1*	*SPC19*	*CDC14*
SPC24	*NKP2*	*SPC34*	
SPC25	*YBP2*	*HSK1*	

Adapted from Biggins et al 2013

B

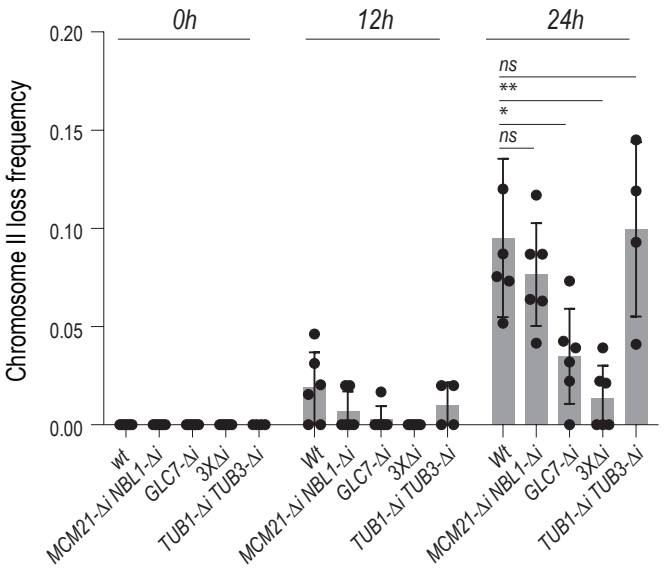

C

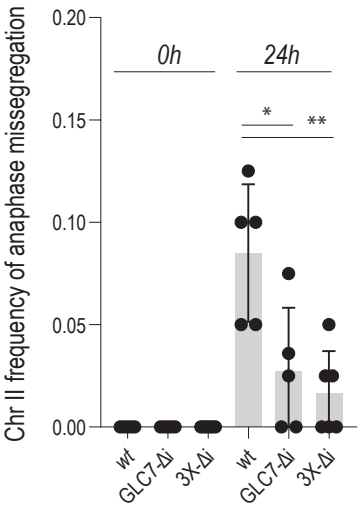

D

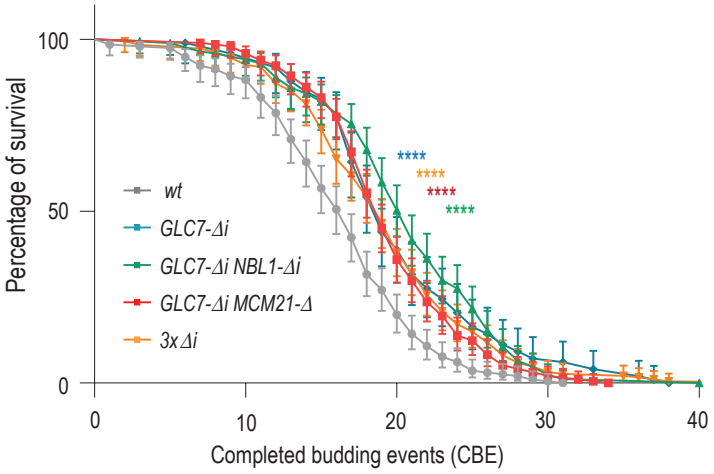

Figure 4

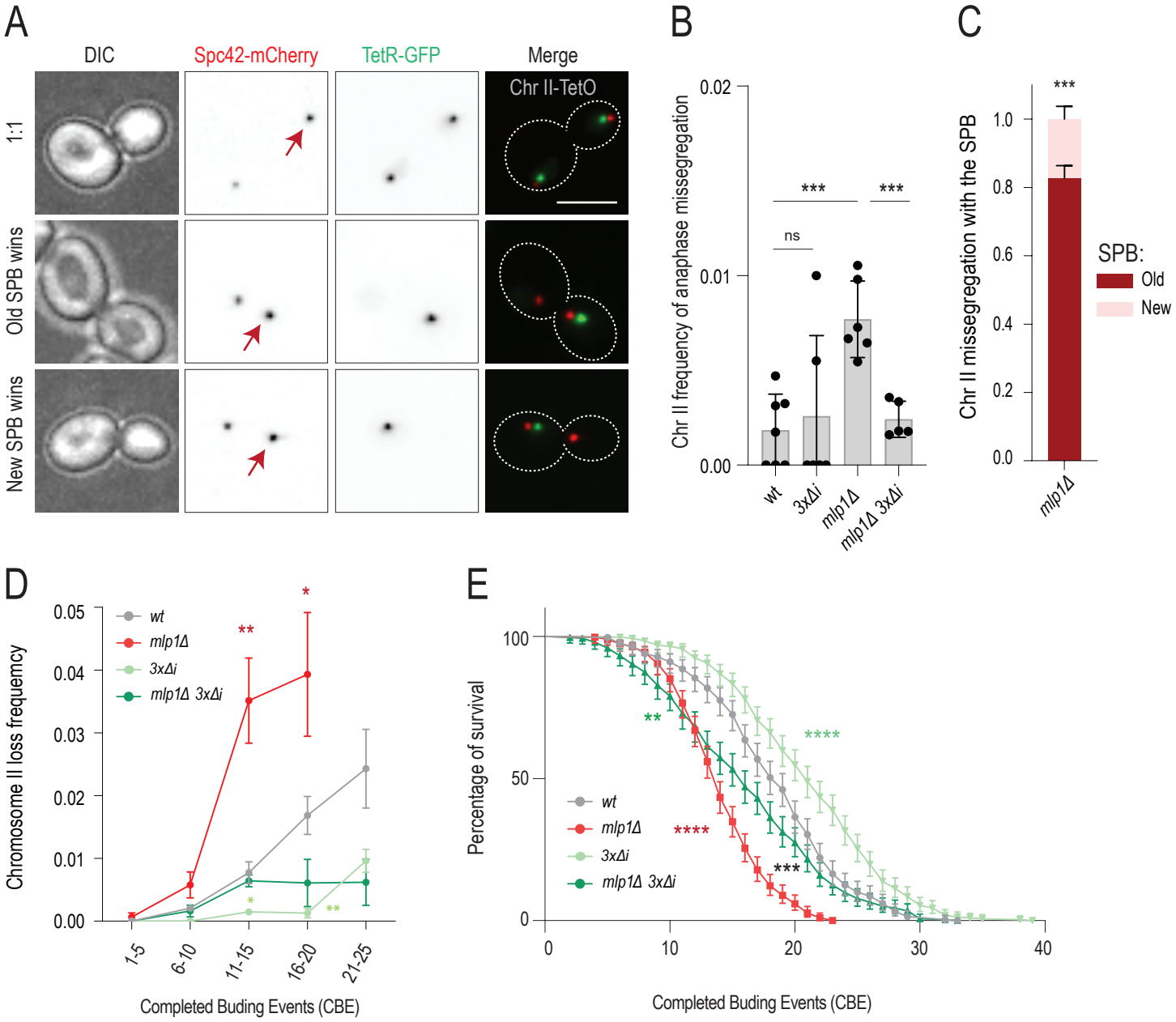
A
DIC
Spc42-mCherry
TetR-GFP
Merge
Chr II-TetO
1:1
Old SPB wins
New SPB wins
B
Chr II frequency of anaphase missegregation
0.02
0.01
0.00
***
***
ns
wt
3xΔi
mlp1Δ
mlp1Δ 3xΔi
C
Chr II missegregation with the SPB
1.0
0.8
0.6
0.4
0.2
0.0
***
SPB:
Old
New
mlp1Δ
D
Chromosome II loss frequency
0.05
0.04
0.03
0.02
0.01
0.00
wt
mlp1Δ
3xΔi
mlp1Δ 3xΔi
**
*
*
**
1-5
6-10
11-15
16-20
21-25
Completed Buding Events (CBE)
E
Percentage of survival
100
50
0
wt
mlp1Δ
3xΔi
mlp1Δ 3xΔi
**
****
****
***
0
10
20
30
40
Completed Buding Events (CBE)

Figure 5

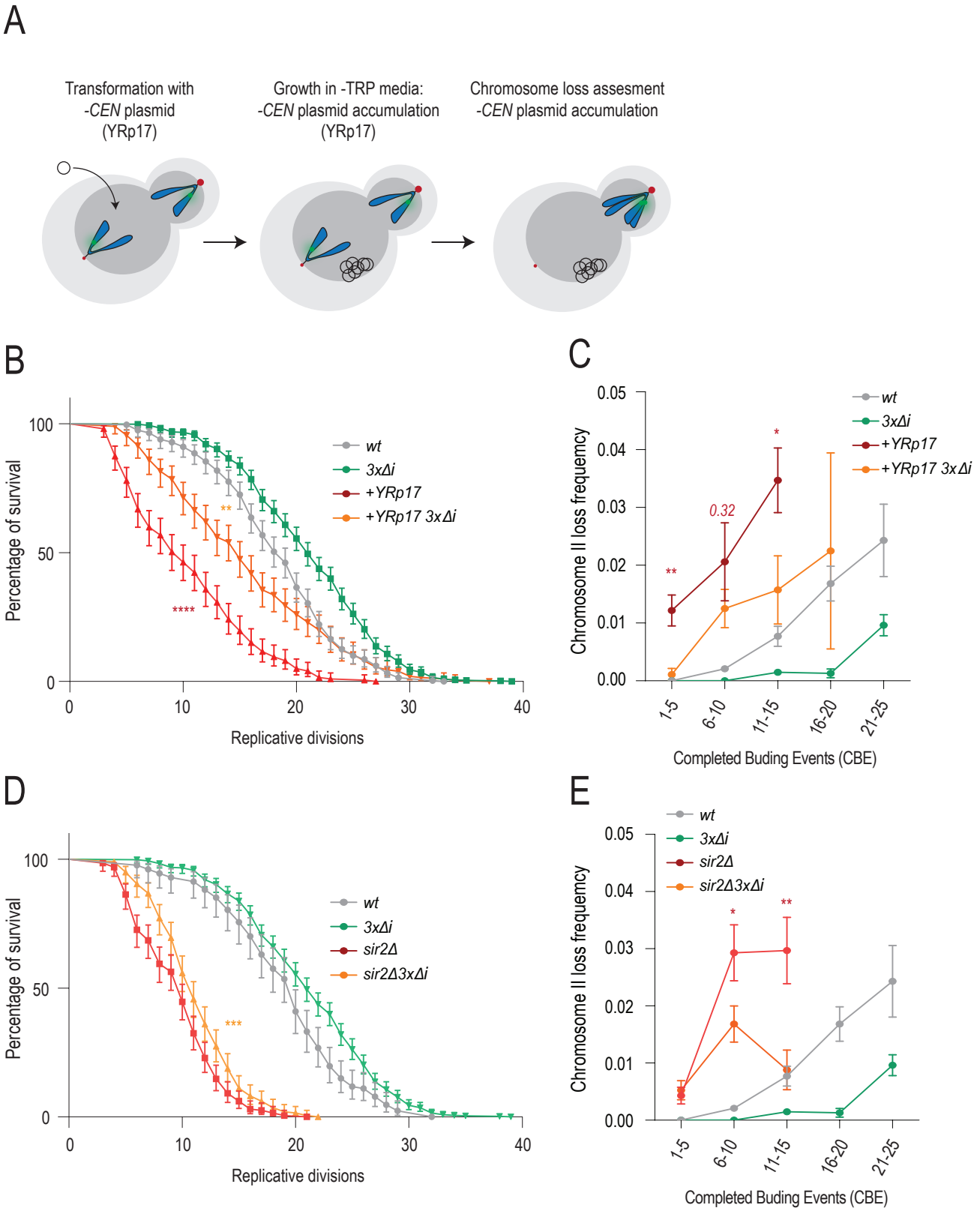
A
Transformation with
-CEN plasmid
(YRp17)
Growth in -TRP media:
-CEN plasmid accumulation
(YRp17)
Chromosome loss assesment
-CEN plasmid accumulation
B
Percentage of survival
Replicative divisions
wt
3xΔi
+YRp17
+YRp17 3xΔi
**
****
C
Chromosome II loss frequency
Completed Buding Events (CBE)
1-5
6-10
11-15
16-20
21-25
0.32
*
**
D
Percentage of survival
Replicative divisions
wt
3xΔi
sir2Δ
sir2Δ3xΔi
***
E
Chromosome II loss frequency
Completed Buding Events (CBE)
wt
3xΔi
sir2Δ
sir2Δ3xΔi
*
**

Figure 6

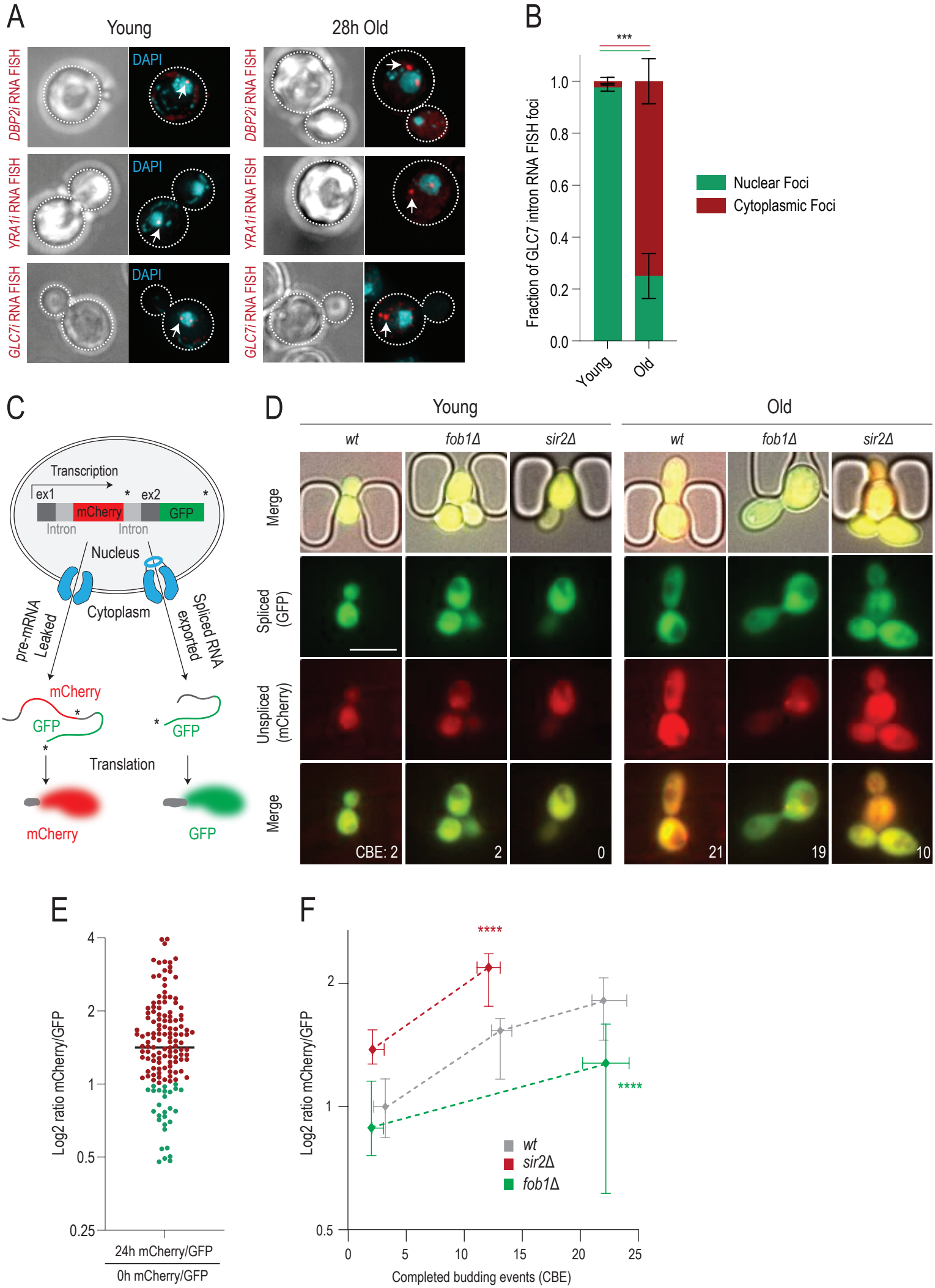
A
Young
28h Old
DBP2i RNA FISH
YRA1i RNA FISH
GLC7i RNA FISH
DAPI
B
***
Fraction of GLC7 intron RNA FISH foci
1.0
0.8
0.6
0.4
0.2
0.0
Young
Old
Nuclear Foci
Cytoplasmic Foci
C
Transcription
ex1
ex2
mCherry
GFP
Intron
Intron
Nucleus
Cytoplasm
pre-mRNA Leaked
Spliced RNA exported
mCherry
GFP
GFP
Translation
mCherry
GFP
D
Young
Old
wt
fob1Δ
sir2Δ
wt
fob1Δ
sir2Δ
Merge
Spliced (GFP)
Unspliced (mCherry)
Merge
CBE: 2
2
0
21
19
10
E
Log2 ratio mCherry/GFP
4
2
1
0.5
0.25
24h mCherry/GFP
0h mCherry/GFP
F
****
****
Log2 ratio mCherry/GFP
2
1
0.5
wt
sir2Δ
fob1Δ
0
5
10
15
20
25
Completed budding events (CBE)

Figure 7

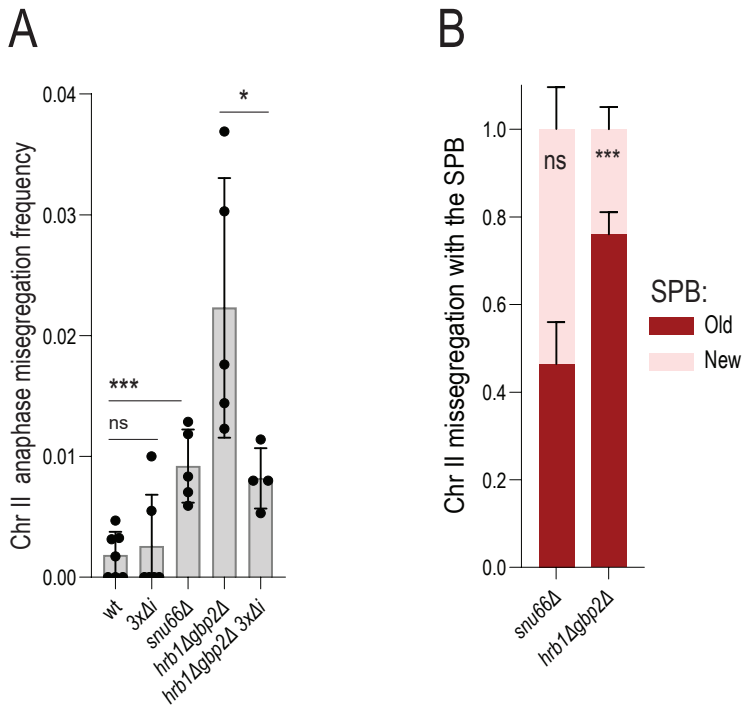
A
B
Chr II anaphase misegregation frequency
0.04
0.03
0.02
0.01
0.00
***
ns
*
wt
3xΔi
snu66Δ
hrb1Δgbp2Δ
hrb1Δgbp2Δ 3xΔi
Chr II missegregation with the SPB
1.0
0.8
0.6
0.4
0.2
0.0
ns
***
snu66Δ
hrb1Δgbp2Δ
SPB:
Old
New

Figure 8

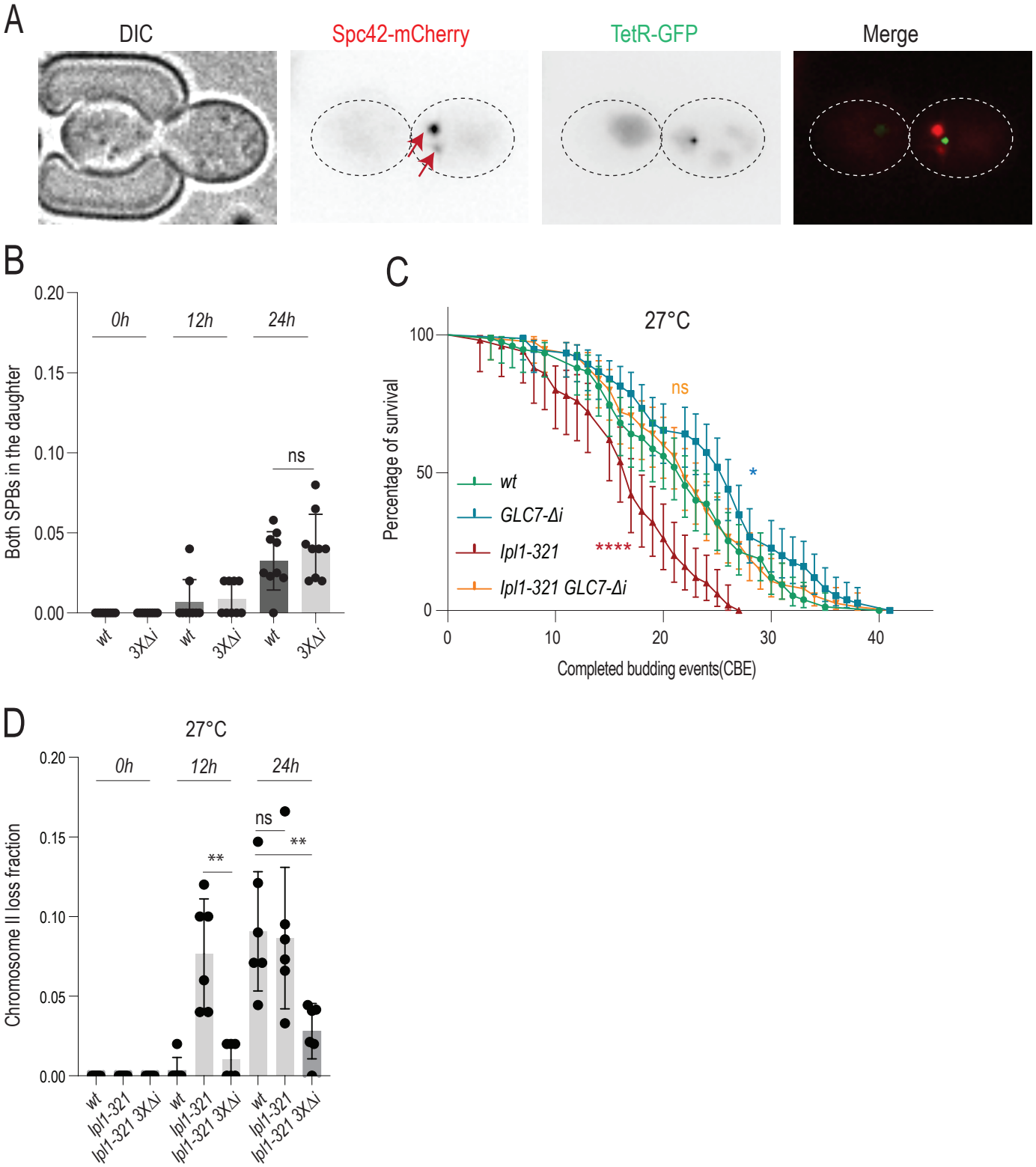

Supplementary Fig 1

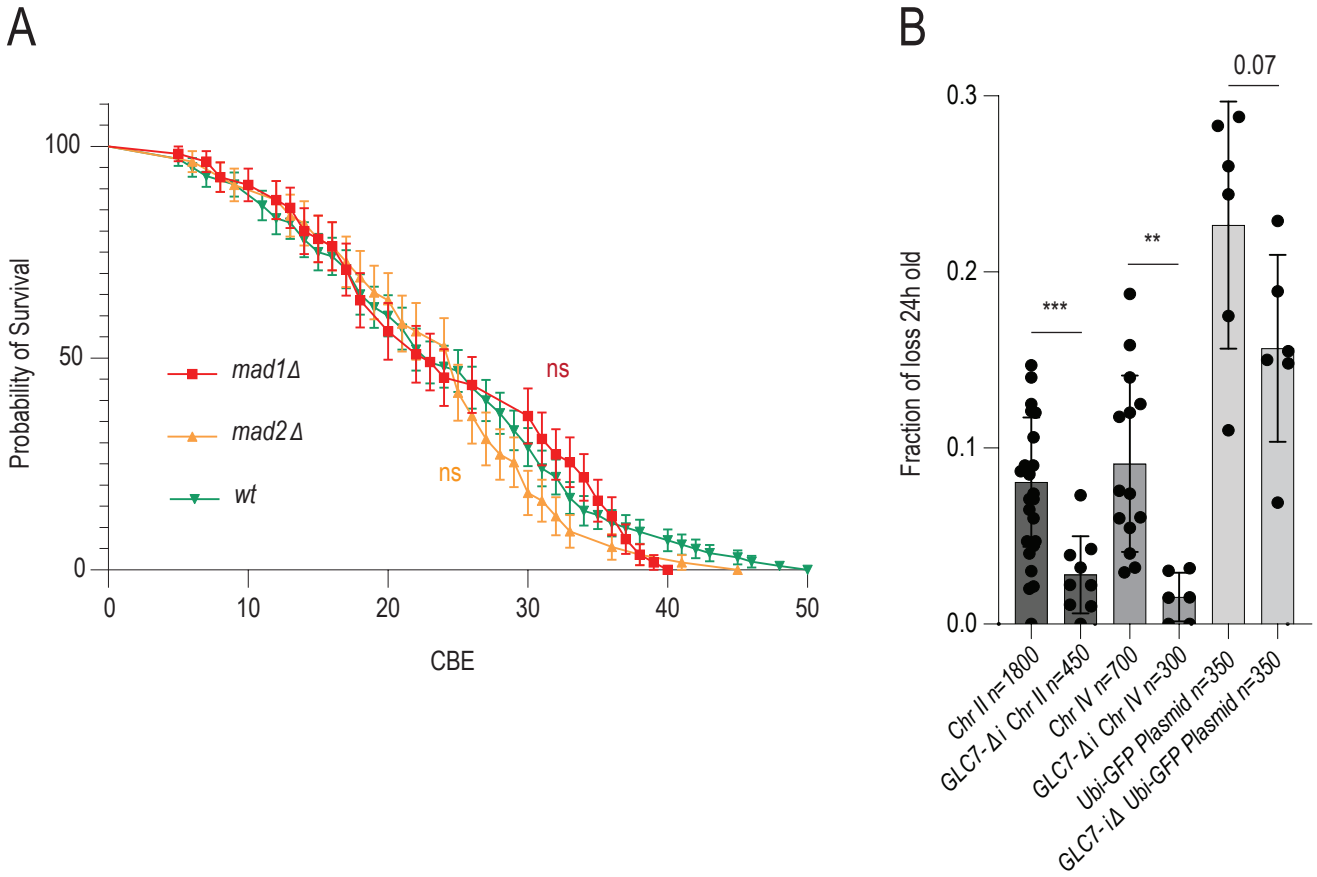

Supplementary Fig 2

A

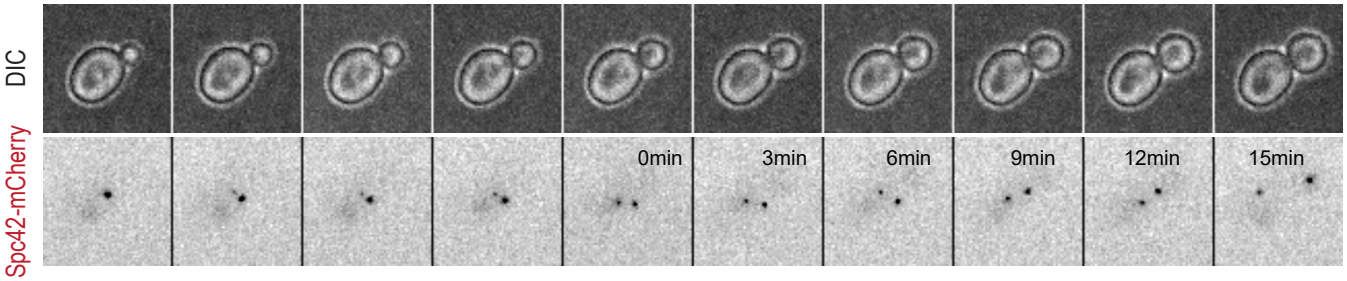

B

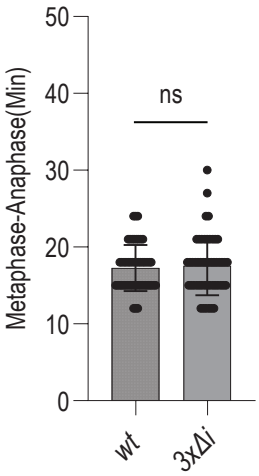

C

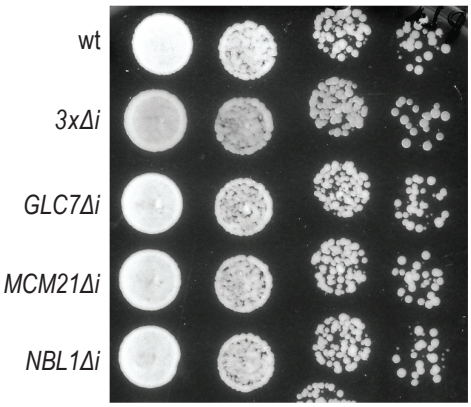

D

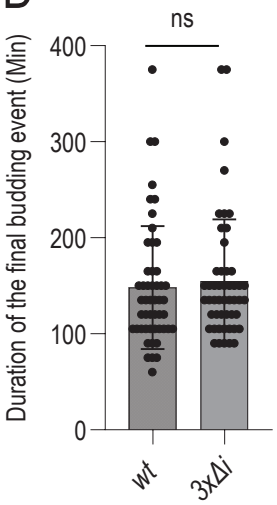

E

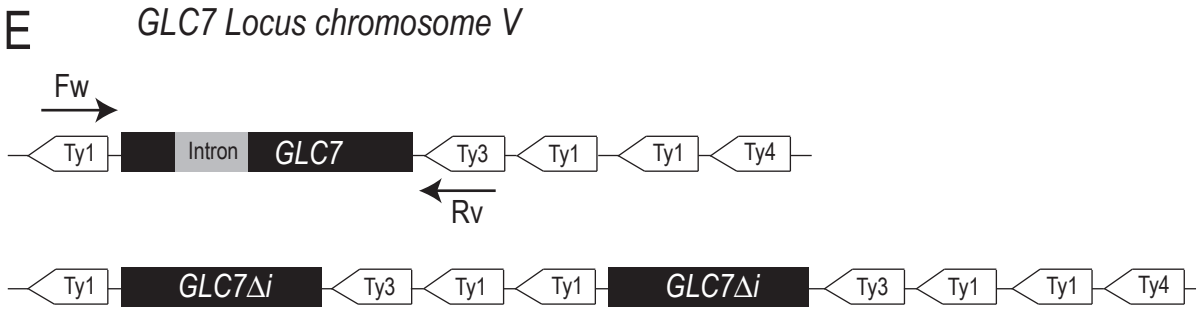

F

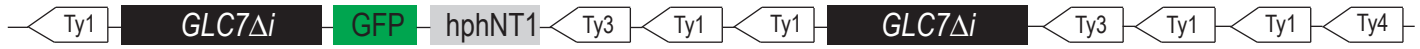

Intron removal results in *GLC7Δi* duplication
C-terminal yeGFP tagging reveals the second copy of *GLC7Δi*

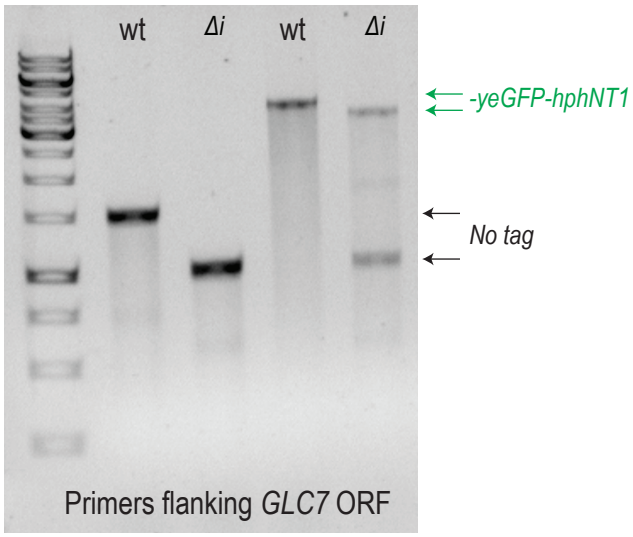

Supplementary Fig 3

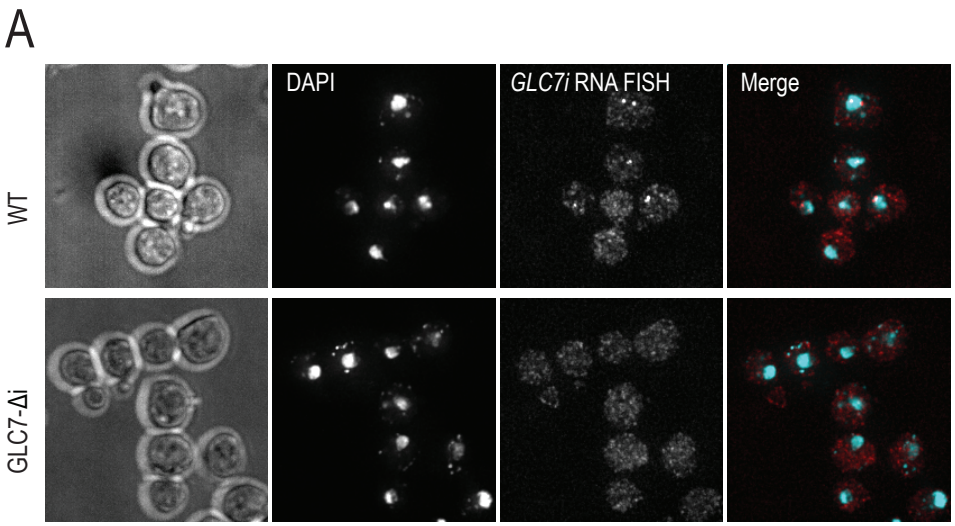

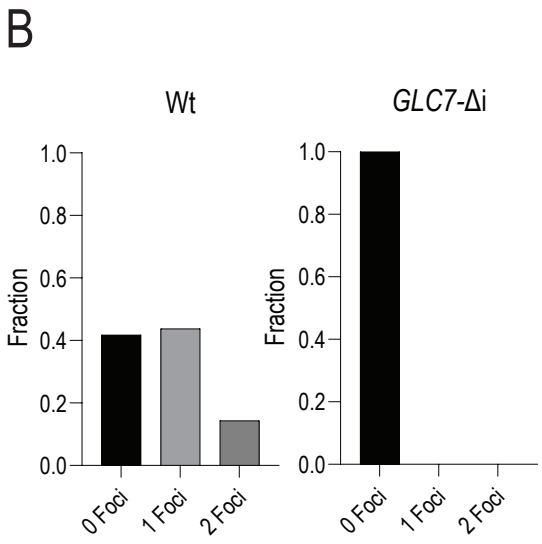

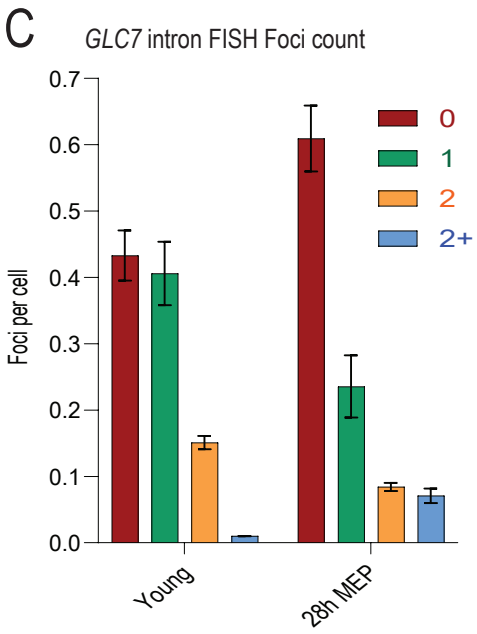

Supplementary Fig 4

YYB number	Genotype	Mating type	Plasmid	Strain made by
962	wt deletion collection	A		Deletion collection
3416	hoD::SCW11pr-Cre-EBD78-NatMX loxP-UBC9-loxP-LEU2 loxP-CDC20-Intron-loxP-HPHMX	α		Dan Gottschling lab
3476	trp1::TetO:TRP1, lys4::LacO:LEU2 ,his3::LacR-GFP:HIS3 ,TetR-RFP	A		Gabriel Neurohr
14507	LEU2::TetR-3mCherry POA1::TetO112:URA3	A		Karsten Weis lab(KWY3759)
16094	Spc42-mCherry:NAT leu2::LEU2 TetR-GFP	A	rec-URA3-CEN-rec-tetO-LEU2	Anna Marzelliusadottir
16128	lys4::LacO:LEU2 his3::LacR-GFP:HIS3 Spc42-mCherry:NAT	α		Anna Marzelliusadottir
16157	trp1::pRS405_Trp1_SplicingReporter	A		Anne Meinema
16161	fob1::KAN, trp1::pRS405_Trp1_SplicingReporter	A		Anne Meinema
16301	sir2::kanMX, trp1::pRS405_Trp1_SplicingReporter	A		Anne Meinema
16648	mad1::kanMX	A		Deletion collection
16934	lys4::LacO:LEU2 his3::LacR-GFP:HIS3 Spc42-mCherry:NAT	A		Mihailo Mirkovic
16935	lys4::LacO:LEU2 his3::LacR-GFP:HIS3 Spc42-mCherry:NAT *lpl1-321*	α		Mihailo Mirkovic
16936	lys4::LacO:LEU2 his3::LacR-GFP:HIS3 Spc42-mCherry:NAT *GLC7-Δi*	A		Mihailo Mirkovic
16937	lys4::LacO:LEU2 his3::LacR-GFP:HIS3 Spc42-mCherry:NAT lpl1-321 *GLC7-Δi*	α		Mihailo Mirkovic
17198	trp1::TetO:TRP1, lys4::LacO:LEU2 ,his3::LacR-GFP:HIS3 ,TetR-mRFP fob1::hphNT1	A		Mihailo Mirkovic
17213	mad2::KanMX	A		Deletion collection
17590	wt elela intronless collection	A	PYB 2665 Ubi-GFP	Mihailo Mirkovic
17591	*GLC7Δi*	A	PYB 2665 Ubi-GFP	Mihailo Mirkovic
17592	*lpl1-321*	α	PYB 2665 Ubi-GFP	Mihailo Mirkovic
17593	*lpl1-321 GLC7Δi*	α	PYB 2665 Ubi-GFP	Mihailo Mirkovic
17677	POA1::TetO112:URA3 leu2::TetR-GFP:LEU2,Spc42-mCherry-hphNT1	α		Mihailo Mirkovic
17678	POA1::TetO112:URA3,leu2::TetR-GFP:LEU2,Spc42-mCherry-hphNT1 *GLC7Δi*	α		Mihailo Mirkovic
17679	POA1::TetO112:URA3,leu2::TetR-GFP:LEU2,Spc42-mCherry-hphNT1 *GLC7/MCM21/NBL1 ΔiΔiΔi*	A		Mihailo Mirkovic
17689	*lpl1-321*	A		Mihailo Mirkovic
17690	*lpl1-321 GLC7Δi*	α		Mihailo Mirkovic
17691	*lpl1-321 MCM21/NBL1ΔiΔi*	A		Mihailo Mirkovic
17692	*lpl1-321 GLC7/MCM21/NBL1-ΔiΔiΔi*	A		Mihailo Mirkovic
17693	wt lpl1 crosses	α		Mihailo Mirkovic
17694	*GLC7Δi*	A		Mihailo Mirkovic
17695	*GLC7/MCM21/NBL1 ΔiΔiΔi*	A		Mihailo Mirkovic
17834	POA1::TetO112:URA3 leu2::TetR-GFP:LEU2,Spc42-mCherry-hphNT1 fob1::Nat	α		Mihailo Mirkovic
17838	POA1::TetO112:URA3 leu2::TetR-GFP:LEU2,Spc42-mCherry-hphNT1 sir2::Nat	α		Mihailo Mirkovic
17924	lpl1-321 Glc7Δi POA1::TetO112:URA3 leu2::TetR-GFP:LEU2 Spc42:mCherry:hphNT1	α		Mihailo Mirkovic
18019	POA1::TetO112:URA3 leu2::TetR-GFP:LEU2 Spc42-mCherry-hphNT	α		Mihailo Mirkovic
18028	POA1::TetO112:URA3 leu2::TetR-GFP:LEU2 Spc42:mCherry:hphNT1	α		Mihailo Mirkovic
18029	lpl1-321 POA1::TetO112:URA3 leu2::TetR-GFP:LEU2 Spc42:mCherry:hphNT	A		Mihailo Mirkovic
18069	POA1::TetO112:URA3 leu2::TetR-GFP:LEU2 Spc42-mCherry-hphNT1	α		Jordan Mccarthy
18070	POA1::TetO112:URA3 leu2::TetR-GFP:LEU2 Spc42-mCherry-hphNT1 hrb1::kan gbp2::kan	α		Jordan Mccarthy
18071	POA1::TetO112:URA3 leu2::TetR-GFP:LEU2 Spc42-mCherry-hphNT1 hrb1::kan gbp2::kan *GLC7/MCM21/NBL1-ΔiΔiΔi*	A		Jordan Mccarthy
18100	POA1::TetO112:URA3 leu2::TetR-GFP:LEU2 Spc42-mCherry-hphNT1 *TUB1/TUB3-ΔiΔi*	A		Mihailo Mirkovic
18100	POA1::TetO112:URA3 leu2::TetR-GFP:LEU2 Spc42-mCherry-hphNT1 *GLC7/MCM21/NBL1-ΔiΔiΔi*	A		Mihailo Mirkovic
18213	POA1::TetO112:URA3 leu2::TetR-GFP:LEU2 Spc42-mCherry-hphNT1 snu66del::Nat	α		Mihailo Mirkovic
18214	POA1::TetO112:URA3 leu2::TetR-GFP:LEU2 Spc42-mCherry-hphNT1 *TUB1/TUB3-ΔiΔi* snu66::Nat	α		Mihailo Mirkovic
18493	POA1::TetO112:URA3 leu2::TetR-GFP:LEU2 Spc42-mCherry-hphNT1 sgf73::Nat	α		Mihailo Mirkovic
18661	POA1::TetO112:URA3 leu2::TetR-GFP:LEU2 Spc42-mCherry-hphNT1 mlp1::nat	α		Mihailo Mirkovic
18663	POA1::TetO112:URA3 leu2::TetR-GFP:LEU2 Spc42-mCherry-hphNT1 mlp1::nat , *GLC7/MCM21/NBL1-ΔiΔiΔi*	A		Mihailo Mirkovic
18683	POA1::TetO112:URA3 leu2::TetR-GFP:LEU2 Spc42:mCherry:hphNT1 *NBL1Δi MCM21Δi*	A		Mihailo Mirkovic
19347	POA1::TetO112:URA3 leu2::TetR-GFP:LEU2 Spc42-mCherry-hphNT1 *GLC7/MCM21/NBL1-ΔiΔiΔi* sir2::Nat	A		Mihailo Mirkovic
19348	POA1::TetO112:URA3 leu2::TetR-GFP:LEU2 Spc42-mCherry-hphNT1 trp1::TetO:TRP1	A		Mihailo Mirkovic
19453	POA1::TetO112:URA3,leu2::TetR-GFP:LEU2,Spc42-mCherry-hphNT1	α	YRp17(PYB546)	Mihailo Mirkovic
19454	POA1::TetO112:URA3,leu2::TetR-GFP:LEU2,Spc42-mCherry-hphNT1 *GLC7/MCM21/NBL1 ΔiΔiΔi*	A	YRp17(PYB546)	Mihailo Mirkovic

Supplementary Table 1